Atmos. Chem. Phys. Discuss.,
https://doi.org/10.5194/acp-2017-839-AC1, 2018

Interactive comment on “Subgrid-scale variability of clear-sky relative humidity and forcing by aerosol-radiation interactions in an atmosphere model” *by* Paul Petersik et al.

Paul Petersik et al.

paul.j.petersik@gmail.com

Received and published: 11 April 2018

Response to Steven Ghan

We thank the reviewer for his constructive comments and for his thorough review. The reviewer comments are in plain font, the authors responses in *Italics*.

General comments

This study introduces stochastic sampling of the PDF of humidity to examine subgrid humidification effects on aerosol radiative forcing. Although this represents an advance over previous estimates of aerosol radiative forcing, important details that

Printer-friendly version

Discussion paper

could substantially influence the results are missing in the description of the treatment. I cannot recommend publication until these details are provided, and only then if the clarified treatment does not substantially bias the results.

The reviewers concerns are to our understanding mostly based on our insufficient description of the aerosol-module HAM2. Therefore, we include a new subsection, "2.1 The aerosol module HAM2" into our methods that briefly summarizes the properties of HAM2.

1. Page 3, lines 23-28. How is the hygroscopicity of each mode determined from the hygroscopicity of each component in the modes?

In ECHAM6-HAM2 the hygroscopicity of internally-mixed aerosols is determined by calculating the volume weighted sum of the κ-values form each soluble compound (see Zhang et al. (2012) section 4.1.3). This is now better explained in the revised paper.

2. Section 2.3 a. How is humidification effect on extinction treated? Extinction is not a simple function of particle radius. See, for example, the method of Ghan and Zaveri (2007). The treatment must be described and justified.

Aerosol radiative properties are calculated using Mie theory. The model uses volume-averaging for each of the seven aerosol modes to calculate the refractive indices where aerosol water is included using the ambient relative humidity. The effective complex radiative indices and the Mie size parameter is then used for the aerosol radiative properties, namely extinction cross section, single scattering albedo, and asymmetry parameter in the radiation scheme (see Zhang et al., 2012, section 2.6).

We thank Dr Ghan for pointing us to this reference, which we now include in the discussion in the revised paper.

b. Does the model treat absorption enhancement by humidification? Some people (Jacobson) think this is quite important.

For the version 2 of the aerosol module HAM the refractive indices for black carbon were updated to reduce the the negative biased aerosol absorption enhancement (Stier et al., 2007). In Stier et al. (2007) it is argued that on a global scale the absorption enhancement of BC due to mixing with hydrophilic aerosols is compensated by the lower life time of and abundance of BC. They base this argument on the study by Stier et al. (2006) where they find that reduced lifetime of BC due to internal mixing actually overbalances the absorption enhancement effect on a global scale such that they observe a decrease in global annual mean clear-sky atmospheric absorption of 0.2 $W\,m^{-2}$. Furthermore, the hypothesis of Jacobson (2012) is very controversial and not supported by most other studies (e.g. Twohy et al., 1989; Chýlek et al., 1996; Liu et al., 2002).

c. Why use the clear-sky value? This biases the estimate of ERFari. Why not include a diagnostic no-aerosol radiation calculation and diagnose ERFari following Ghan (2013)?

We followed the advice of the referee. We now present our results in terms of a radiative forcing due to aerosol-radiation interactions (RFari) that is calculated as suggested by Ghan (2013). As one would expect, RFari changes less (from -0.15 to -0.19 $W\,m^{-2}$, ∼31%) due to the masking effect of clouds than $ERFari_{cls}$ (from -0.29 to -0.45 $W\,m^{-2}$, ∼57%) in response to the implementation of our parameterization. However, we still *observe a clear signal that the implementation of our parameterization enhances the cooling by the direct aerosol effect.*

3. Page 7, last paragraph. Your argument about scattering vs absorption would be stronger if you compare the impact on AOD with the impact on AAOD. It is likely that the sensitivity of ERFari is biased by your treatment of humidification effects on absorption and by neglecting contributions from cloudy sky.

We have included two variables into the Table 1, namely AAOD and AAOD by black carbon. We see a positive change in AAOD $+0.12 \cdot 10^{-3}$ *(*$\sim$ *4.7%). However, AOD changed in absolute values by nearly two orders of magnitude more, namely* $+ 9.0 \cdot 10^{-3}$ *(*$\sim$ *7.8%).*

References

Chýlek, P., Lesins, G. B., Videen, G., Wong, J. G. D., Pinnick, R. G., Ngo, D., and Klett, J. D.: Black carbon and absorption of solar radiation by clouds, J. Geophys. Res., 101, 23 365–23 371, doi:10.1029/96JD01901, 1996.

Ghan, S. J.: Technical Note: Estimating aerosol effects on cloud radiative forcing, Atmos. Chem. Phys., 13, 9971–9974, doi:10.5194/acp-13- 9971-2013, 2013.

Ghan, S. J. and Zaveri, R. A.: Parameterization of optical properties for hydrated internally mixed aerosol, J. Geophys. Res., 112, D10 201, doi:10.1029/2006JD007927, 2007.

Jacobson, M. Z.: Investigating cloud absorption effects: Global absorption properties of black carbon, tar balls, and soil dust in clouds and aerosols, J. Geophys. Res., 117, D06 205, doi:10.1029/2011JD017218, 2012.

Liu, L., Mishchenko, M. I., Menon, S., Macke, A., and Lacis, A. A.: The effect of black carbon on scattering and absorption of solar radiation by cloud droplets, Journal of Quantitative Spectroscopy and Radiative Transfer, 74, 195–204, doi:10.1016/S0022-4073(01)00232-1, 2002.

Stier, P., Seinfeld, J. H., Kinne, S., Feichter, J., and Boucher, O.: Impact of nonabsorbing anthropogenic aerosols on clear-sky atmospheric absorption, J. Geophys. Res., 111, D18 201, doi:10.1029/2006JD007147, 2006.

Stier, P., Seinfeld, J. H., Kinne, S., and Boucher, O.: Aerosol absorption and radiative forcing, Atmospheric Chemistry and Physics, 7, 5237–5261, 2007.

Twohy, C. H., Clarke, A. D., Warren, S. G., Radke, L. F., and Charlson, R. J.: Light-absorbing material extracted from cloud droplets and its effect on cloud albedo, J. Geophys. Res., 94, 8623–8631, doi:10.1029/JD094iD06p08623, 1989.

Zhang, K., O'Donnell, D., Kazil, J., Stier, P., Kinne, S., Lohmann, U., Ferrachat, S., Croft, B., Quaas, J., Wan, H., Rast, S., and Feichter, J.: The global aerosol-climate model ECHAM-HAM, version 2: sensitivity to improvements in process representations, Atmos. Chem. Phys., 12, 8911–8949, doi:10.5194/acp-12-8911-2012, 2012.

Interactive comment on Atmos. Chem. Phys. Discuss., https://doi.org/10.5194/acp-2017-839, 2017.

Atmos. Chem. Phys. Discuss.,
https://doi.org/10.5194/acp-2017-839-AC2, 2018

Interactive comment on "Subgrid-scale variability of clear-sky relative humidity and forcing by aerosol-radiation interactions in an atmosphere model" *by* Paul Petersik et al.

Paul Petersik et al.

paul.j.petersik@gmail.com

Received and published: 11 April 2018

Response to Reviewer 2

We thank the reviewer for his/her constructive comments and for his/her thorough review. The reviewer comments are in plain font, the responses in *Italics*.

General comments

This study applied a stochastic parameterization of subgrid-scale variability of relative humidity (RH) to a global climate-aerosol model, ECHAM6-HAM2, and examined the impact of the subgrid-scale variability of RH on aerosol optical depth (AOD) and radiative forcing. The authors showed the subgrid-scale variability of RH increased global mean aerosol hygroscopic growth, AOD (by 7.8%), and effective radiative forcing (by 57%) due to the non-linear response of hygroscopic growth to RH. Although this study showed a slight improvement of the estimation of AOD, I don't think this study is suitable for a paper of Atmospheric Chemistry and Physics because the scientific findings, methods, and analysis of this study are not enough as shown below.

To emphasize the scientific importance of applying a stochastic parameterization to clear-sky relative humidity for its application in the aerosol hygroscopic growth scheme we now highlight better in the revised manuscript that our study is the first study that is proposed without strong simplifications about the shape of the used probability density function (PDF) and that is consistent with the cloud cover scheme. This is discussed in more detail further down in this authors response.
Furthermore, we also emphasize in the revision the point that applying a stochastic parameterization is not only a method to estimate uncertainties but leads to a better representation of the mean state of the atmosphere. This was recently summarized in Berner et al. (2017). To highlight this in an example we refer to Tompkins and Berner (2008) that use a method of subgrid-scale variability that is very similar to ours. They investigate its influence when it is applied on the convective scheme of the European Centre for Medium-Range Weather Forecasts (ECMWF) ensemble prediction system. They show that their new stochastic convective scheme generally improves the skill of the operational system for most variables in the short to medium range in mid-latitudes.

Main comments

1) Page 2, lines 7-27
These two paragraphs describe about previous studies. I understand from these paragraphs that the underestimation of radiative forcing by using the grid-box mean RH is

already recognized well in previous studies. In addition, there are some global model studies focused on the subgrid-scale variability of RH previously. Due to these two points, it is hard to understand what was advanced scientifically in this study. This study is new in ECHAM6-HAM2, but I feel that there is no clear advancement both scientifically and technically in the community of aerosol and cloud studies.

We gather that the reviewer refers to our discussion of the studies of Haywood and Shine (1997) and Haywood and Ramaswamy (1998) which apply a subgrid-scale variability of RH in a GCM. We regret that in the previous manuscript version obviously we did not clarify well enough that our study goes substantially beyond this previous work.
1. Haywood and Shine (1997) investigated the effect of subgrid-scale variability in an idealized case. They use globally for each grid cell and height level five fixed RH-values that are taken from a normal distribution around RH = 70%. Hence, they show the gross effect of subgrid-scale variability of RH but do not propose a scheme that is meant to be integrated into an atmosphere model.
2. Haywood and Ramaswamy (1998) use a more sophisticated approach by computing the subgrid-scale variability based on a triangular shaped distribution around grid-box mean RH. However, the shape and width of the distribution is globally constant. In our parameterization the width of the PDF is a function of height (Quaas, 2012). Furthermore, the PDF that Haywood and Ramaswamy implement is artificially generated and inconsistent with the assumptions in the cloud scheme. In contrast, we sample the sub-saturated part of the PDF from the cloud-cover scheme.
Haywood and Shine (1997) and Haywood and Ramaswamy (1998) have in common that they just investigate the effects on RFari by sulphate. We investigate the effect on the entire radiative forcing of aerosols that are included in the ECHAM6-HAM2 model. Summarizing, our study is the first study that investigated the effect of subgrid-scale variability in an approach that does not make idealized assumptions and that is consistent with the cloud cover scheme.

In response to the reviewer comment, the sentence: "Haywood and Shine (1997) and Haywood and Ramaswamy (1998) include a subgrid-scale variability of RH for the calculation of RFari by sulphate."
in lines 17f of the original manuscript has been amended as follows:
"First attempts to implement a subgrid-scale variability of RH in a GCM for the calculation of RFari by sulphate were made by Haywood and Shine (1997) and Haywood and Ramaswamy (1998). However, these studies make strong simplifications about the shape of the used probability density function (PDF) and are not consistent with the cloud cover scheme."

2) Section 2.2
Please explain why the stochastic treatment was used. Does this mean only single RH value is calculated by Eq. (6) and used in each grid box and each time? I think considering the full range of RH (shown in Figure 1) in each grid box and time is not so difficult, for example by using 5-10 RH bins between RHcls - delta RHcls and RHcls + delta RHcls. This will not increase the computational cost of the model so much. If a random RH is used in the model, does it assure the repeatability of model simulations? For example, when the authors make two simulations which use completely the same inputs and model setups, can the authors obtain the same results from the two simulations?

At each time step and each grid box we apply Eq. (6) using a newly generated random number. This is computationally cheaper than subsampling the entire PDF in each time step while on average one expects a very similar result. It should be noted that our scheme is intended for use in a 3-D climate model and not just constructed to show that taking into account subgrid scale variability decreases ERFari. Applying a binning approach for the RH values means, in other words, increasing the resolution of the model for the hygroscopic growth scheme. This results in additional computational

Printer-friendly version

Discussion paper

cost compared with the approach suggested here.
Up until now, we used a random number generator that starts always with a new seed. In general it would be possible to start always with the same seed. The repeatability of our study is ensured by integrating the model over a rather long time (10 years). Hence, we expect to find results that do not differ from our results larger than within the given error bars (95%). In the current setting, the integration is not fully deterministic anymore. We clarify this now in the revised text.

3) Treatment of aerosol absorption
How does the model calculate aerosol absorption? Please describe the method and the treatment of absorption enhancement by water. The treatment of absorption enhancement of black carbon by water will be a key in the calculations of single scattering albedo and radiative forcings. The authors show negative values of radiative forcings, but I suspect the authors do not consider the positive forcings by the absorption enhancement. The absolute values of radiative forcings will be smaller when the absorption enhancement is treated properly, and the total effect of the subgrid-scale variability of RH will be less important.

Aerosol radiative properties are calculated using Mie theory. The model uses volume-averaging for each of the seven aerosol modes to calculate the refractive indices where aerosol water is included using the ambient relative humidity. The effective complex radiative indices and the Mie size parameter is then used for the aerosol radiative properties, namely extinction cross section, single scattering albedo, and asymmetry parameter in the radiation scheme (see Zhang et al. (2012) section 2.6). The explanation is now extended in the revised manuscript.
For the version 2 of the aerosol module HAM the refractive indices for black carbon were updated to reduce the negative bias aerosol absorption enhancement (Stier et al., 2007). Based on findings of Stier et al. (2006) it is argued in Stier et al. (2007)

that the absorption enhancement of BC due to mixing with hydrophilic aerosols is compensated by the lower life time of and abundance of BC.

In contrast to Jacobson (2012) and Bond et al. (2013), HAM2 does not include a very strong absorption enhancement for absorbing particles inside clouds. This is because the hypothesis of Jacobson (2012) is very controversial and not supported by most other studies (e.g. Twohy et al., 1989; Chýlek et al., 1996; Liu et al., 2002).

We include values for the AAOD and AAOD of BC. In PD simulations AAOD increases by +0.12 ($\pm$0.4) $\cdot$ 10^{-3} ($\sim$ 4.7%) were the AAOD by BC increased by +0.11 ($\pm$0.3) $\cdot$ 10^{-3} ($\sim$5.1%). This shows that our parameterization leads to a stronger absorption of solar light by BC aerosols. However, the overall increase of AOD in PD simulations due to our new parameterization is +9.0 ($\pm$2.2) $\cdot$ 10^{-3} ($\sim$7.8%). That highlights that in our simulations the contribution of absorption to AOD is rather low although absorption is enhanced.

For point 3, the reviewers concerns are to our understanding mostly based on our insufficient description of the aerosol-module HAM2. Therefore, we include a new subsection, "2.1 The aerosol module HAM2" into our methods that briefly summarizes the properties of HAM2.

Other comments

Page 1, lines 23-24:

I think Ginoux [2017] is for mineral dust only. References for primary and secondary organic aerosols and aerosols from biomass burning should be added.

We included Bond et al.(2013) and Myhre et al. (2013) for biomass burning, Shindell et al. (2013) for SOA as well as a reference to the AR5 from the IPCC.

Page 2, line 7:
"However" is better to move to the next sentence (before "General circulation").

Changed.

Page 2, lines 34-35:
I cannot understand what the authors mean in this sentence ("RHcls is chosen. . .") and next sentence ("That means, . . ."). I don't think "aerosol-radiation interactions are negligible in the cloud part". Some studies (e.g. Jacobson) have shown the importance of this issue.

In the standard configuration ECHAM6-HAM2 uses the mean clear-sky relative humidity ($\overline{RH}_{\mathrm{cls}}$) instead of the grid-box mean relative humidity ($\overline{RH}$) to compute aerosol hygroscopic growth. Note, that $\overline{RH}_{\mathrm{cls}}$ is by definition smaller than $\overline{RH}$:

$$\overline{RH} = f \cdot \overline{RH}_{\mathrm{cloud}} + (1-f) \cdot \overline{RH}_{\mathrm{cls}} = f + (1-f) \cdot \overline{RH}_{\mathrm{cls}}$$

Here, f is the fractional cloud cover. It is assumed that the radiative effect of the hygroscopic growth of aerosol is more important in the cloud-free part than for interstitial aerosol in clouds where cloud radiative effects are dominant. If not RH_{cls} but $\overline{RH}$ would be used to calculate the aerosol hygroscopic growth for the entire grid-box, aerosols would grow to strong in the cloud free part where aerosol-radiation interactions are of higher importance than in the cloudy sky. Thus, it is reasoned in the ECHAM literature to use RH_{cls} instead $\overline{RH}$ (see section 2.6 in Stier et al., 2005).
We added to the method section:
"RH_{cls} is chosen, instead of grid-box mean relative humidity RH, because cloud processing and cloud radiative effects are dominant in the cloudy part of a grid box as reasoned in Stier et al. (2005) for ECHAM5-HAM1."

Page 3, line 28:

I don't think "age due to internal mixing" is good explanation. Did the authors mean that internally-mixed particles are made by aging processes such as condensation and coagulation?

Yes, that is what we meant. We changed the sentence to:
"DU and BC are considered as non-hygroscopic on emission. However, they can merge with hygroscopic particles due to internal mixing by ageing processes such as condensation and coagulation."

Page 4, line 15:

Because the authors used "usually" here, it looks there are some previous studies considering the subgrid-scale variability.

We just want to highlight that the idea of subgrid-scale variability is not new to model formulations (e.g. vertical velocity) but was not applied (besides in idealized studies as mentioned further up) in global circulation models to RH or RH_{cls}. We deleted the "usually" changed the sentence to:
"Several global atmosphere models including ECHAM6-HAM2 already make assumptions to account for the subgrid-scale variability of atmospheric variables, e.g. for vertical velocity when computing droplet activation rates (Ghan et al., 1997; Lohmann et al., 2007; Golaz et al., 2011). However, subgrid-scale variability of RH or RH_{cls} is not taken into account when computing hygroscopic growth of interstitial aerosols besides in some studies that made gross simplification regarding the shape and variation of the used PDF (Haywood and Shine, 1997; Haywood and Ramaswamy 1998)."

Page 4, Line 25:

The values of cs, ct, and nx should be given after the equation (2) (at line 8).

Changed.

Page 5, line 2:
What is “Rhcls,old”?

We changed the expression to $\overline{RH}_{\text{cls}}$. *This variable is used earlier to indicate the grid-box mean clear-sky relative humidity that was actually meant by* $RH_{\text{cls,old}}$.

Page 6, line 6:
“c” values (Equation (9)) are not useful in the current manuscript. Discuss more or remove from the manuscript.

We agree with the referee and removed them from the manuscript.

Page 6, line 13:
How important the different growth factors between CS/AS and KS/NS modes is?

In Figure 2a one can see that particles swell stronger for bigger aerosol modes due to the implementation of the new parameterization. For more clarity, we changed the sentence:
“Thus, the effect is stronger for particles from CS and AS mode than for particles from KS and NS mode. “
to:
“Thus, the effect is strongest for particles from the CS mode (red line in Fig. 2a) and

Printer-friendly version

Discussion paper

weakest for particles from the NS mode (black line in Fig. 2a)"

Page 6, line 18:
Why did AOD increase especially in the tropics?

Our parameterization leads to an on average stronger growth of hygroscopic aerosols, especially for very hygroscopic aerosols that are sulphate and sea salt.
Sea salt is most abundant in lower latitudes in the model. This is indicated in Figure 1 that we attached to this response. Depicted is the AOD by non-hydrated sea salt aerosols. Furthermore, anthropogenic emissions of sulphate are very high in China, India and over the Arab Peninsula and contribute in addition to the peak of increased AOD in the northern tropics.

Page 6, line 25:
Why don't you show the results of "c" by using a figure?

We excluded the c-value completely from the paper in response to the previous reviewer comment on "Page 6, line 6".

Page 6, line 29:
"w" means single scattering albedo?

Yes. But we use term "ratio of scattering to total extinction" when we refer to results from the radiation transfer equation to compute the ratio between scattering/extinction. We do this in order to make the mentioned variable clearly distinguishable from the single scattering albedo as a property of a certain particle type (that is constant).

Page 6, line 32:
The alpha change shown here is for wet particles? Please clarify. Please show the percentage of the change.

Yes it is the parameter for wet particles. We added this and the percentage of this change.

Page 7, line 14:
Did the authors show the definition of ERFaer?

We added a description of how ERFaer was computed.

What is the difference between ERFari-cls and ERFaer?

In response to the comments of Steven Ghan, we now discuss our results in terms of radiative forcing due to aerosol-radiation interactions (RFari) to avoid confusion due to the earlier used $ERFari_{cls}$*, that was a idealized value that depicted the radiative inbalance at the top of atmosphere in a hypothetical atmosphere without clouds.*

The effect of total and anthropogenic aerosols is shown, respectively?

We just show the ERF due to anthropogenic aerosols (ERFaer) since we compute the difference between PD and PI emissions. We now mention this in the methods section in the manuscript.

Printer-friendly version

Discussion paper

Page 7, line 15:
Why did cloud cover increase in PD simulations but decrease in PI simulations?

We ascribe this to internal variability. That can be seen by overlapping confidence intervals:
TCC_{PD}: -0.08 $\pm$ 0.14%
TCC_{PI}: 0.17 $\pm$ 0.14%

We added a sentence about internal variability to the discussion.

Page 9, line 13:
The authors focus on sulfate and sea salt here, but how about nitrate, ammonium, and secondary organic aerosol? How does the global model treat these aerosol species?

We focus on sulphate and sea salt because they are very hygroscopic (for HAM2 κ_{SS} = 1.12 and κ_{SO4} = 0.6, see Zhang et al., 2012) in comparison to SOA (κ_{SOA} = 0.037). Aerosols that are more hygroscopic are more sensitive to changes in relative humidity than aerosols that are less hygroscopic. This characteristic is what we use for the explanation of the observed profile of the change in the growth factor. Note, that the κ-value for sulphate in HAM2 is in the range of the observed value for ammonium sulphate (0.33 - 0.72) (Petters and Kreidenweise, 2007). Furthermore, the model that we use currently does not simulate nitrate aerosols (Stier et al., 2005). We highlight in our paper now that the addition of nitrate aerosols will introduce very hygroscopic aerosols into the model that would alter our results.

Page 10, lines 1-5:
Please show the simulation results obtained by the authors rather than citing previous

studies.

We now integrate a profile plot that shows that the mixing ratio of hygroscopic aerosols. The plot shows that the mixing ratio of sea salt decreases stronger with height than for other aerosols. Hence, the overall aerosols composition becomes less hygroscopic.

Page 10, line 8:
Please explain why the function of height is used. The authors explain the treatment in the cloud scheme but do not explain whether the treatment is realistic.

RH_{crit} is a function of height in the general formulation of ECHAM6-HAM2. Implicitly we already stated that in the introduction when we referred to Quaas (2012). However, now clearly formulate that Quaas (2012) found RH_{crit} to be a function of height.

Page 10, line 11:
"Eq. (Equation 1)" should be "Eq. (1)".

Changed.

References

Berner, J., Achatz, U., Batté, L., Bengtsson, L., Cámara, A. d. I., Christensen, H. M., Colangeli, M., Coleman, D. R. B., Crommelin, D., Dolaptchiev, S. I., Franzke, C. L. E., Friederichs, P., Imkeller, P., Järvinen, H., Juricke, S., Kitsios, V., Lott, F., Lucarini, V., Mahajan, S., Palmer, T. N., Penland, C., Sakradzija, M., von Storch, J.-S., Weisheimer, A., Weniger, M., Williams, P. D., and Yano, J.-I.: Stochastic Parameterization: Toward a New View of Weather and Climate Models, Bull. Amer. Meteor. Soc., 98, 565–588, doi:10.1175/BAMS-D- 15-00268.1, 2016.

Bond, T. C., Doherty, S. J., Fahey, D. W., Forster, P. M., Berntsen, T., DeAngelo, B. J., Flanner, M. G., Ghan, S., Kärcher, B., Koch, D., Kinne, S., Kondo, Y., Quinn, P. K., Sarofim, M. C., Schultz, M. G., Schulz, M., Venkataraman, C., Zhang, H., Zhang, S., Bellouin, N., Guttikunda, S. K., Hopke, P. K., Jacobson, M. Z., Kaiser, J. W., Klimont, Z., Lohmann, U., Schwarz, J. P., Shindell, D., Storelvmo, T., Warren, S. G., and Zender, C. S.: Bounding the role of black carbon in the climate system: A scientific assessment, J. Geophys. Res. Atmos., 118, 5380–5552, doi:10.1002/jgrd.50171, 2013.

Ghan, S. J., Leung, L. R., Easter, R. C., and Abdul-Razzak, H.: Prediction of cloud droplet number in a general circulation model, J. Geophys. Res., 102, 21 777–21 794, 1997.

Golaz, J.-C., Salzmann, M., Donner, L. J., Horowitz, L. W., Ming, Y., and Zhao, M.: Sensitivity of the aerosol indirect effect to subgrid variability in the cloud parameterization of the GFDL Atmosphere General Circulation Model AM3, J. Clim., 24, doi:10.1175/2010JCLI3945.1, 2011.

Haywood, J. M. and Ramaswamy, V.: Global sensitivity studies of the direct radiative forcing due to anthropogenic sulfate and black carbon aerosols, J. Geophys. Res., 103, 6043–6058, doi:10.1029/97JD03426, 1998.

Haywood, J. M. and Shine, K. P.: Multi-spectral calculations of the direct radiative forcing of tropospheric sulphate and soot aerosols using a column model, Q.J.R. Meteorol. Soc., 123, 1907–1930, doi:10.1002/qj.49712354307, 1997.

Jacobson, M. Z.: Investigating cloud absorption effects: Global absorption properties of black carbon, tar balls, and soil dust in clouds and aerosols, J. Geophys. Res., 117, D06 205, doi:10.1029/2011JD017218, 2012.

Lohmann, U., Stier, P., Hoose, C., Ferrachat, S., Kloster, S., Roeckner, E., and Zhang, J.: Cloud microphysics and aerosol indirect effects in the global climate model ECHAM5-HAM, 7, 3425–3446, 2007.

Liu, L., Mishchenko, M. I., Menon, S., Macke, A., and Lacis, A. A.: The effect of black carbon on scattering and absorption of solar radiation by cloud droplets, Journal of Quantitative Spectroscopy and Radiative Transfer, 74, 195–204, doi:10.1016/S0022-4073(01)00232-1, 2002.

Myhre, G., Samset, B. H., Schulz, M., Balkanski, Y., Bauer, S., Berntsen, T. K., Bian, H., Bellouin, N., Chin, M., Diehl, T., Easter, R. C., Feichter, J., Ghan, S. J., Hauglustaine, D., Iversen, T., Kinne, S., Kirkevåg, A., Lamarque, J.-F., Lin, G., Liu, X., Lund, M. T., Luo, G., Ma, X., van Noije, T., Penner, J. E., Rasch, P. J., Ruiz, A., Seland, o., Skeie, R. B., Stier, P., Takemura, T., Tsigaridis, K., Wang, P., Wang, Z., Xu, L., Yu, H., Yu, F., Yoon, J.-H., Zhang, K., Zhang, H., and Zhou, C.: Radiative forcing of the direct aerosol effect from AeroCom Phase II simulations, Atmospheric Chemistry and Physics, 13, 1853–1877, doi:10.5194/acp-13-1853-2013, 2013.

Petters, M. D. and Kreidenweis, S. M.: A single parameter representation of hygroscopic growth and cloud condensation nucleus activity, Atmos. Chem. Phys., 7, 1961–1971, doi:10.5194/acp-7-1961-2007, 2007.

Quaas, J.: Evaluating the “critical relative humidity” as a measure of subgrid-scale variability of humidity in general circulation model cloud cover parameterizations using satellite data, J. Geophys. Res., 117, D09 208, doi:10.1029/2012JD017495, 2012.

Shindell, D. T., Lamarque, J.-F., Schulz, M., Flanner, M., Jiao, C., Chin, M., Young, P. J., Lee, Y. H., Rotstayn, L., Mahowald, N., Milly, G., Faluvegi, G., Balkanski, Y., Collins, W. J., Conley, A. J., Dalsoren, S., Easter, R., Ghan, S., Horowitz, L., Liu, X., Myhre, G., Nagashima, T., Naik, V., Rumbold, S. T., Skeie, R., Sudo, K., Szopa, S., Takemura, T., Voulgarakis, A., Yoon, J.-H., and Lo, F.: Radiative forcing in the ACCMIP historical and future climate simulations, Atmos. Chem. Phys., 13, 2939–2974, doi:10.5194/acp-13-2939-2013, 2013.

Stier, P., Feichter, J., Kinne, S., Kloster, S., Vignati, E., Wilson, J., Ganzeveld, L., Tegen, I., Werner, M., Balkanski, Y., Schulz, M., Boucher, O., Minikin, A., and Petzold, A.: The aerosol-climate model ECHAM5-HAM, Atmos. Chem. Phys., 5, 1125–1156, doi:10.5194/acp-5- 1125-2005, 2005.

Stier, P., Seinfeld, J. H., Kinne, S., Feichter, J., and Boucher, O.: Impact of nonabsorbing anthropogenic aerosols on clear-sky atmospheric absorption, J. Geophys. Res., 111, D18 201, doi:10.1029/2006JD007147, 2006.

Stier, P., Seinfeld, J. H., Kinne, S., and Boucher, O.: Aerosol absorption and radiative forcing, Atmospheric Chemistry and Physics, 7, 5237–5261, 2007.

Tompkins, A. M. and Berner, J.: A stochastic convective approach to account for model uncertainty due to unresolved humidity variability, J. Geophys. Res., 113, D18 101, doi:10.1029/2007JD009284, 2008.

Twohy, C. H., Clarke, A. D., Warren, S. G., Radke, L. F., and Charlson, R. J.: Light-absorbing material extracted from cloud droplets and its effect on cloud albedo, J. Geophys. Res., 94, 8623–8631, doi:10.1029/JD094iD06p08623, 1989.

Zhang, K., O'Donnell, D., Kazil, J., Stier, P., Kinne, S., Lohmann, U., Ferrachat, S., Croft, B., Quaas, J., Wan, H., Rast, S., and Feichter, J.: The global aerosol-climate model ECHAM-HAM, version 2: sensitivity to improvements in process representations, Atmos. Chem. Phys., 12, 8911–8949, doi:10.5194/acp-12-8911-2012, 2012.

Interactive comment on Atmos. Chem. Phys. Discuss., https://doi.org/10.5194/acp-2017-839, 2017.

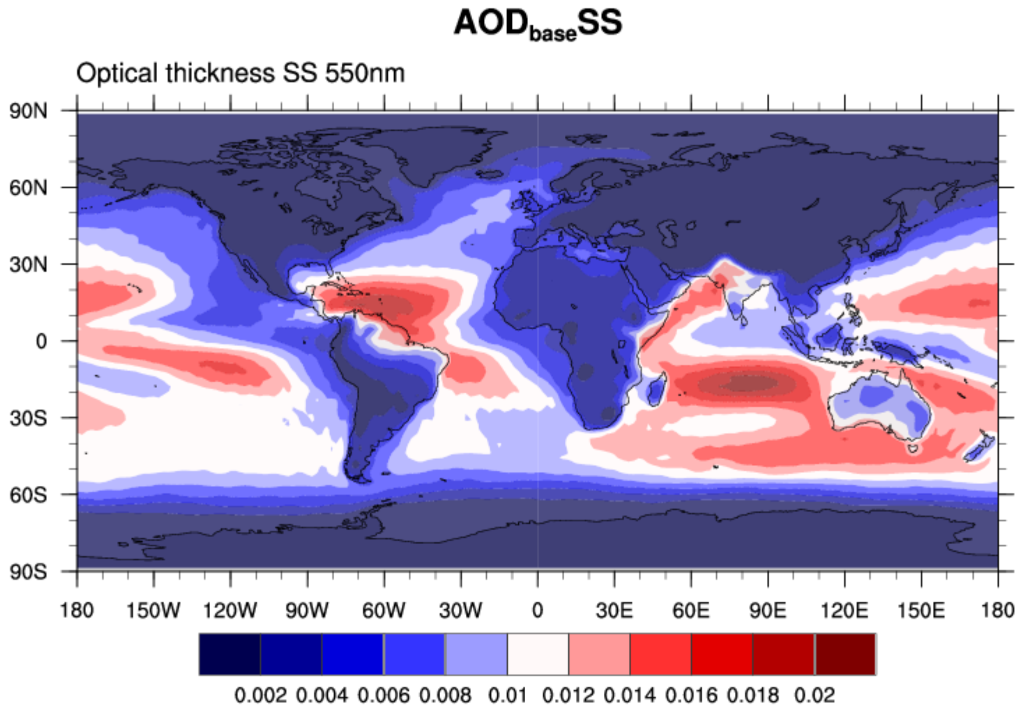

Fig. 1. AOD by sea salt (SS) in the control run of the model.

Printer-friendly version

Discussion paper

List of relevant changes

Page and line numbers are given for the marked-up manuscript version.

Page 1, line 9f
We excluded the statement:

"The ability of the model to simulate AOD is slightly improved with respect to satellite data from MODIS-Aqua."

Page 1, line 12f
Results are now presented in terms of RFari instead of ERFari_cls.

Page 1, line 24
We included literature for the radiative forcing by different aerosol compounds.

Page 2, line 14ff
We moved the following sentence to the end of the paragraph.

"In addition, recent studies show that models with a coarse resolution which do not take subgrid-scale variability of various aerosol properties into account underestimate aerosol radiative forcing (Gustafson et al., 2011) and have a significant negative bias in aerosol optical depth (Weigum et al., 2016) ."

Page 2, line 19ff
We included a more detailed description about Haywood and Shine (1997) and Haywood and Ramaswamy (1998) to show that our study goes substantially beyond this previous work.

Page 3, line 16ff
We included a paragraph about Tompkins and Berner (2008) to show a successful application of a method of subgrid-scale variability of humidity that is very similar to ours.

Page 3, line 27ff
We included an entire subsection about the aerosol module HAM2. We now explain in more detail how HAM2 calculates refractive indices and treats absorption enhancement of BC.

Page 4, line 23ff
We included statements about the hygroscopicity of nitrate, ammonium and internally-mixed aerosols in HAM2.

Page 4, line 30ff
We explain in more detail why HAM2 uses in its standard setup RH_cls instead RH in the hygroscopic growth scheme.

Page 4, Table 1
We included a table for the kappa values as they are used in HAM2.

Page 5, line 8ff
The paragraph about aerosol modes is moved to the new subsection about the module HAM2.

Page 7, line 3f
We included a sentence about the repeatability of our study.

Page 7, line 10ff
We included the definition of the total ERF by anthropogenic aerosols, ERFaer, that we use, excluded the definition of ERFari_cls and included the definition of RFari.

Page 8, line 12ff
We excluded the discussion of our model results in terms of the variable “c” from the entire manuscript.

Page 8, line 19ff
The statement about the confidence interval is moved from page 8, line 28f to page 8, line 19ff.

Page 9, line 3ff
Again, we excluded the discussion of our model results in terms of the variable “c”.

Page 9, line 8ff
We included results for the absorption aerosol optical depth.

Page 9, line 16ff
We moved the results regarding cloud cover from page 9, line 35ff to page 9, line 16ff.

Page 9, line 29f
Results are now presented in terms of RFari instead if ERFari_cls.

Page 11, Table 2
We included results for RFari, AOD_WAT, AAOD and AAOD_BC. We removed the results for ERFari_cls.

Page 12, line 8f
We included a statement about the profile of the mixing ratio of soluble aerosol compounds to underline our argument made in point (2).

Page 13, line 13ff
We included an explanation why the effect of the new parameterization is especially strong for lower latitudes.

Page 14, Figure 1b
We included a figure depicting the profile of the mixing ratio of various aerosol compounds.

Page 14, line 1f
We included a sentence regarding the internal variability of cloud cover in our model.

Page 14, line 9f
We now briefly highlight the advances of our study in respect to previous studies in the conclusions.

Page 14, line 5f
We excluded the comparison of our results to data from MODIS-Aqua.

Subgrid-scale variability of clear-sky relative humidity and forcing by aerosol-radiation interactions in an atmosphere model

Paul Petersik[1], Marc Salzmann[1], Jan Kretzschmar[1], Ribu Cherian[1], Daniel Mewes[1], and Johannes Quaas[1]

[1]Leipzig Institute for Meteorology, Universität Leipzig

Correspondence to: Paul Petersik (paul.j.petersik@gmail.com)

Abstract. Atmosphere models with resolutions of several tens of kilometres take subgrid-scale variability of the total specific humidity q_t into account by using a uniform probability density function (PDF) to predict fractional cloud cover. However, usually only mean relative humidity, $\overline{\mathrm{RH}}$, or mean clear-sky relative humidity, $\overline{\mathrm{RH}}_{\mathrm{cls}}$, is used to compute hygroscopic growth of soluble aerosol particles. In this study, a stochastic parameterization of subgrid-scale variability of $\mathrm{RH}_{\mathrm{cls}}$ is applied. For this, we sample the subsaturated part of the uniform RH-PDF from the cloud cover scheme for ~~application in association with~~ its application in the hygroscopic growth parameterization in the ECHAM6-HAM2 atmosphere model. Due to the non-linear dependence of the hygroscopic growth on RH, this causes an increase in aerosol hygroscopic growth. Aerosol optical depth (AOD) increases by a global mean of 0.009 (~~$\sim 7.8\,\%$~~ $\sim 7.8\,\%$ in comparison to the control run). Especially over the tropics AOD is enhanced with a mean of about 0.013. ~~The ability of the model to simulate AOD is slightly improved with respect to satellite data from MODIS-Aqua.~~ Due to the increase in AOD, net top of the atmosphere clear-sky solar radiation, $SW_{\mathrm{net,cls}}$, decreases by $-0.22\,\mathrm{W\,m^{-2}}$ (~~$\sim -0.08\,\%$~~$\sim -0.08\,\%$). Finally, the ~~effective~~ radiative forcing due to aerosol-radiation interactions ~~under clear-sky conditions (ERFari$_{\mathrm{cls}}$~~(RFari) changes from ~~-0.29~~$-0.15\,\mathrm{W\,m^{-2}}$ ~~to -0.45~~to $-0.19\,\mathrm{W\,m^{-2}}$ by about ~~57~~31 %. The reason for this very disproportionate effect is that anthropogenic aerosols are disproportionally hygroscopic.

1 Introduction

Aerosols have a significant impact on the climate system by interacting with radiation and clouds. Solar and thermal radiation interact with aerosols by absorption and scattering processes. Despite extensive research on atmospheric aerosols, the effective radiative forcing due to aerosol-radiation interactions (ERFari) has still a large uncertainty. The ERFari combines effects from radiative forcing due to aerosol-radiation interactions (RFari) and rapid adjustments and is estimated to be -0.45 (-0.95 to $+0.05$) $\mathrm{W\,m^{-2}}$ by the 5th assessment report (AR5) of the Intergovernmental Panel on Climate Change (IPCC) (Boucher et al., 2013). The radiative forcing by aerosol-radiation interactions from sulphate ($-0.4\,\mathrm{W\,m^{-2}}$) and nitrate ($-0.11\,\mathrm{W\,m^{-2}}$) is a cooling effect on the radiative balance of the Earth due to increased scattering of solar radiation. In contrast, black carbon ($+0.4\,\mathrm{W\,m^{-2}}$) is warming the Earth's climate due to absorption of solar radiation. Additionally, it is uncertain if primary and secondary organic aerosols, aerosols from biomass burning and mineral dust have a net cooling or a warming effect ~~(Ginoux, 2017)~~ (e.g. Bond et al., 2013; Shindell et al., 2013; Myhre et al., 2013; Ginoux, 2017) . In total, anthropogenic aerosols have very likely a cooling effect through aerosol-radiation interactions on the radiative balance of the Earth (Boucher et al., 2013).

Through ~~various~~ non-linear relationships described by Beer-Lambert's law (Lambert, 1760; Beer, 1852) and Mie scattering (Mie, 1908), the extinction of radiation is related to the aerosol particle radius. The aerosol particle radius of hygroscopic aerosols like sulphate or sea salt aerosols increases in a humid environment due to attraction of water. This hygroscopic growth is a non-linear function of the ambient relative humidity (RH), where hygroscopic growth is especially enhanced close to saturation (Köhler, 1936). Therefore, extinction due to hygroscopic aerosols increases strongly when the humidity of the ambient air approaches saturation (Zieger et al., 2013; Skupin et al., 2016; Haarig et al., 2017).

~~However, it~~ It is known that humidity varies on subgrid scales in ~~global circulation models~~ general circulation models (GCMs) with largest subgrid-scale variability in the middle troposphere ~~(Quaas, 2012) . General circulation models (GCMs)~~(e.g. Quaas (2012)). However, GCMs that just use the grid-box mean relative humidity $\overline{\mathrm{RH}}$ to calculate hygroscopic growth of aerosols do not take this subgrid-scale variability of humidity and its effect on radiation into account. Various studies show that GCMs underestimate the RFari of sulphate aerosols by 30 to 80 % when not considering subgrid-scale variability of RH for the hygroscopic growth of sulphate particles (Haywood et al., 1997; Petch, 2001; Myhre et al., 2002). ~~In addition, recent studies show that models with a coarse resolution which do not take subgrid-scale variability of various aerosol properties into account underestimate aerosol radiative forcing (Gustafson et al., 2011) and have a significant negative bias in aerosol optical depth (Weigum et al., 2016) . The mentioned~~ These studies use high resolution models and compare the results from calculations of radiative forcing that keep the high resolution of RH with either calculation where RH is averaged spatially beforehand to mimic a GCM resolution or results from model configurations with a coarser resolution. In addition, recent studies show that models with a coarse resolution which do not take subgrid-scale variability of various aerosol properties into account underestimate aerosol radiative forcing (Gustafson et al., 2011) and have a significant negative bias in aerosol optical depth (Weigum et al., 2016) .

~~Haywood and Shine (1997) and Haywood and Ramaswamy (1998) include~~ First attempts to implement a subgrid-scale variability of RH in a GCM for the calculation of RFari by sulphate ~~directly into GCM simulations~~were made by Haywood and Shine (1997) and Haywood and Ramaswamy (1998) . However, these studies make strong simplifications about the shape of the used probability density function (PDF) and are not consistent with the cloud cover scheme. Haywood and Shine (1997) prescribe the RH distribution globally for clear skies. Here, for each grid cell and height level five fixed RH-values are taken from a normal distribution around RH$=70$ %. They find that RFari by sulphate is 24% greater than the non-hydrated forcing when using the grid-box mean RH. However, RFari by sulphate increases up to 37% when the subgrid-scale variability of RH is applied and the correlation between clouds and areas of high relative humidity is taken into account. Hence, RFari by sulphate increased by about 10% from simulations that use grid-box mean RH to simulations with a subgrid-scale variability of RH. Haywood and Ramaswamy (1998) have a more sophisticated approach. They use a triangular shaped relative humidity distribution around the grid-box mean RH with a magnitude of ±10% that is truncated at RH=1.0 as proposed by Haywood et al. (1997). ~~However, the authors emphasize that they do not consider variations of width and shape of the used distribution. In their study~~In this study, RFari by sulphate is enhanced by 9% due to the subgrid-scale variability of RH when ~~including clouds~~ clouds are included. We want to point out that Haywood and Ramaswamy (1998) do not consider variations of width and shape of the used distribution.

In this study, we implement a stochastic parameterization of subgrid-scale variability of clear-sky relative humidity $\mathrm{RH_{cls}}$ into the global aerosol-climate model of the Max Planck Institute for Meteorology (MPI-M) ECHAM6-HAM2 ~~(Zhang et al., 2012)~~ (Zhang For this, we use a uniform probability density function (PDF) that reproduces the subsaturated part of the cloud cover scheme from Sundqvist et al. (1989) that is used by ECHAM6 (Stevens et al., 2013). The width of the PDF from the cloud cover scheme is a function of height (Quaas, 2012; Rosch et al., 2015) . Hence, our parameterization inherits this feature. ECHAM6-HAM2 until now used the grid box-mean clear-sky relative humidity $\overline{\mathrm{RH}}_{\mathrm{cls}}$ ~~in the cloud free part of the model~~ to calculate hygroscopic growth (Zhang et al., 2012). ~~$\overline{\mathrm{RH}}_{\mathrm{cls}}$ is chosen, instead of grid-box mean relative humidity $\overline{\mathrm{RH}}$, because cloud processing and cloud radiative effects are dominant in the cloudy part of a grid box. That means, aerosol-radiation interactions are negligible in the cloud part.~~ Now, rather than using the grid-box mean, the PDF of the subgrid-scale variability of $\mathrm{RH_{cls}}$ is randomly sampled for each time step, grid cell and height level to compute the growth factor *gf* (see section 2). Hygroscopic growth is computed in ECHAM6-HAM2 for all hygroscopic aerosol constituents that are incorporated in the model. Therefore, the effect subgrid-scale variability of $\mathrm{RH_{cls}}$ on hygroscopic growth is included for all hygroscopic aerosol particles in the model. ~~In we investigate~~

A very similar method of subgrid-scale variability of humidity is for example applied on the convective scheme of the European Centre for Medium-Range Weather Forecasts (ECMWF) ensemble prediction system by Tompkins and Berner (2008) . They show that their new stochastic convective scheme generally improves the skill of the operational system for most variables in the short to medium range in the mid-latitudes. More generally, we want to emphasize that stochastic parameterizations are not only a method to estimate uncertainties but lead to a better representation of the mean state of the atmosphere. This was recently summarized in Berner et al. (2016) .

In section 2 of this article we describe the aerosol module HAM2 in more detail and introduce our stochastic parameterization of clear-sky relative humidity. Then, we investigate in section 3 how the new parameterization changes optical and radiative properties of the atmosphere. Afterwards, the results are discussed in section 4. Finally, this study is summarized with an outlook for further research in section 5.

2 Methods

2.1 ~~Hygroscopic growth in ECHAM6-HAM2~~ Aerosol Module HAM2

~~Hygroscopic~~ In this section, we briefly describe the aspects of the micro-physical aerosol module HAM2 (Zhang et al., 2012) that are relevant for this study. The micro-physical aerosol module HAM2 is the successor of its first version that was introduced by Stier et al. (2005) . HAM2 is built as an extension of the atmospheric general circulation model ECHAM6 (Stevens et al., 2013) . It incorporates the following aerosol components: Sulphate (SO4), black carbon (BC), organic carbon (OC), sea salt (SS) and mineral dust (DU). The module predicts the evolution of the aerosol population based on 7 log-normal modes (4 soluble (S) and 3 insoluble (I)) that describe the size distribution of atmospheric aerosol. The modes are divided into Nucleation (N,

$r < 0.005$ µm), Aitken (K, $0.005 < r < 0.05$ µm), Accumulation (A, $0.05 < r < 0.5$ µm) and Coarse (C, $r > 0.5$ µm) mode and are abbreviated in the following such as CS for soluble Coarse mode. The main soluble aerosol constituents are SS, SO4 and OC. DU and BC are considered as insoluble on emission. However, insoluble aerosols can become soluble if they merge with soluble particles due to internal mixing by ageing processes such as condensation and coagulation (Vignati et al., 2004) .

Aerosol radiative properties are calculated for 24 spectral bands for shortwave and 16 bands for longwave radiation using Mie theory by applying the algorithm suggested by Toon and Ackerman (1981) . The model uses the volume-weighted average refractive indices for internally mixed aerosols where aerosol water is included (Stier et al., 2005; Ghan and Zaveri, 2007) . The effective complex radiative indices and the Mie size parameter are then used for the aerosol radiative properties, namely extinction cross section, single scattering albedo, and asymmetry parameter in the radiation scheme. For the version 2 of the aerosol module the refractive indices for black carbon were updated to reduce the the negative bias due to aerosol absorption enhancement (Stier et al., 2007) . Based on findings of Stier et al. (2006) it is argued in Stier et al. (2007) that the absorption enhancement of BC due to mixing with hydrophilic aerosols is compensated by the lower life time and abundance of BC. In contrast to Jacobson (2012) and Bond et al. (2013) , HAM2 does not include a very strong absorption enhancement for absorbing particles inside clouds. It should be noted that the hypothesis of Jacobson (2012) is very controversial and not supported by most other studies (e.g. Twohy et al., 1989; Chýlek et al., 1996; Liu et al., 2002) .

Hygroscopic growth HAM2

Soluble particles can grow in size due to the attraction of water. This hygroscopic growth can be described by the growth factor $gf = r_{\mathrm{wet}}/r_{\mathrm{dry}}$, where r_{wet} and r_{dry} are the wet and dry radius of an aerosol particle, respectively. Petters and Kreidenweis (2007) introduced the κ-Köhler theory to calculate the growth factor as a function of relative humidity and temperature

$$\frac{\mathrm{RH}}{\exp\left(\frac{A_{\mathrm{K}}(T)}{D_{\mathrm{dry}}\,gf}\right)} = \frac{gf^3 - 1}{gf^3 - (1-\kappa)} \qquad (1)$$

where RH is the ambient relative humidity, D_{dry} the dry diameter, A_{K} the temperature-dependent parameter of the Kelvin (curvature) effect and κ the hygroscopicity. A κ value of 0 describes completely hydrophobic aerosols, whereas κ values greater than 0.5 describe very hygroscopic aerosols. ~~Common aerosol constituents with~~ Aerosol constituents with very high κ values ~~are sulphate~~ in HAM2 are sulphate and sea salt (see Table 1). Note that the κ value for sulphate in HAM2 is in the range of the observed value for ammonium sulphate (0.33 - 0.72) ~~, nitrate (~ 0.8) and sea spray (0.91 - 1.33) (Zhang et al., 2012)~~ (Petters and Kreidenweis, 2007) . Furthermore, HAM2 does not include nitrate in its current set-up. The hygroscopicity of internally-mixed aerosols is determined by calculating the volume-weighted average of the κ-values form each soluble compound. In Eq. (1) gf is a strictly-monotonically increasing, non-linear function with positive curvature for $\mathrm{RH} \in [0,1]$.

ECHAM6-HAM2 uses the grid-box mean clear-sky relative humidity $\overline{\mathrm{RH}}_{\mathrm{cls}}$ in Eq. (1) to calculate the hygroscopic growth for each aerosol mode. $\overline{\mathrm{RH}}_{\mathrm{cls}}$ is chosen, instead of grid-box mean relative humidity $\overline{\mathrm{RH}}$, because $\overline{\mathrm{RH}}_{\mathrm{cls}}$ is a better estimate for the relative humidity in the cloud-free part of a grid cell than $\overline{\mathrm{RH}}$ and cloud processing and cloud radiative effects are

Table 1. κ-values as used in HAM2 from Zhang et al. (2012) . The κ-value for sulphate in HAM2 is in the range of the observed value for Ammonium sulphate (Petters and Kreidenweis, 2007) . Furthermore, HAM2 does not include nitrate in its current set-up.

Compound	κ
Sulphate	0.60
Sea salt	1.12
Primary organic aerosol	0.06
Secondary organic aerosol	0.022 - 0.070
Black carbon	0
Mineral dust	0
Nitrate	-

dominant in the cloudy part of a grid box as reasoned in Stier et al. (2005) for ECHAM5-HAM1. This means that since the aerosol-radiation interactions have a small effect compared to the cloud reflectivity in the cloudy part of a grid cell, swelling is only approximately treated in the cloudy part. $\overline{\mathrm{RH}}_{\mathrm{cls}}$ is diagnosed from predicted $\overline{\mathrm{RH}}$. For this, saturation is assumed in clouds ($\mathrm{RH} = 1$). When the grid-box is cloud-free ($f = 0$) or partly cloudy ($0 < f < 1$), clear-sky relative humidity is computed by $\overline{\mathrm{RH}}_{\mathrm{cls}} = \left(\overline{\mathrm{RH}} - f\right)/(1 - f)$ where f is the fractional cloud cover. For overcast grid-boxes ($f = 1$), the clear-sky relative humidity is ~~not defined and~~ set to saturation as well ($\overline{\mathrm{RH}}_{\mathrm{cls}} = 1$). Using the $\overline{\mathrm{RH}}_{\mathrm{cls}}$ in Eq. (1) implies that no subgrid-scale variability of $\mathrm{RH}_{\mathrm{cls}}$ is used beyond the information supplied by the fractional cloud cover.

~~The aerosol module HAM2 calculates hygroscopic growth for each aerosol mode. There are 7 log-normal (4 soluble (S) and 3 insoluble (I)) modes to describe the size distribution of atmospheric aerosol. The modes are divided into Nucleation (N, $r < 0.005$m), Aitken (K, $0.005 < r < 0.05$m), Accumulation (A, $0.05 < r < 0.5$m) and Coarse (C, $r > 0.5$m) mode and are abbreviated in the following such as CS for soluble Coarse mode. The main hygroscopic aerosol constituents are sea salt (SS), sulphate (SO4) and organic carbon (OC). Mineral dust (DU) and black carbon (BC) are considered as non-hygroscopic on emission but may age due to internal mixing.~~

2.2 Stochastic parameterization for the subgrid-scale variability of clear-sky relative humidity

In the ECHAM model, subgrid-scale variability of specific humidity is already used for the prediction of fractional cloud cover (Stevens et al., 2013). The cloud scheme assumes a uniform probability density function (PDF) as proposed by Sundqvist et al. (1989) for the horizontal subgrid-scale variability of total-water q_{t} between $\bar{q}_{\mathrm{t}} - \Delta q$ and $\bar{q}_{\mathrm{t}} + \Delta q$, where $\Delta q = \gamma q_{\mathrm{s}}$ (see Fig. 1a). $\bar{q}_{\mathrm{t}}$ is the model-predicted grid-box mean total-water specific humidity and q_{s} the saturation specific humidity computed from the predicted grid-box mean temperature. The scaling parameter γ is varying in the vertical but otherwise assumed to be constant in space and time. It can be calculated by $\gamma = 1 - \mathrm{RH}_{\mathrm{crit}}$, where $\mathrm{RH}_{\mathrm{crit}}$ is the critical relative humidity that is a function of height (Quaas, 2012; Rosch et al., 2015). Fractional cloud cover occurs if the grid box mean relative humidity $\overline{\mathrm{RH}}$

exceeds the critical relative humidity. In ECHAM6-HAM2, $\mathrm{RH_{crit}}$ is parametrized as a ~~function of height~~ by

$$\mathrm{RH_{crit}}(p) = c_\mathrm{t} + (c_\mathrm{s} - c_\mathrm{t})\exp\left[1 - \left(\frac{p_\mathrm{s}}{p}\right)^{n_\mathrm{x}}\right] \tag{2}$$

with p the ambient pressure and p_s the surface pressure~~and c_t and c_s~~. Furthermore, $c_\mathrm{t} = 0.7$ and $c_\mathrm{s} = 0.9$ are the critical relative humidity values at the top of the atmosphere (TOA) and the surface, respectively~~.~~

, and $n_x = 4$. The given values for c_t, c_s and n_x are the same as in the in the cloud cover scheme of ECHAM6. While the formulation of $\mathrm{RH_{crit}}$ is specific to the ECHAM6 model, the cloud cover scheme from Sundqvist et al. (1989) has also been applied in other global models. Furthermore, the Tiedtke (1993) cloud cover scheme which is for example used in the Geophysical Fluid Dynamics Laboratory (GFDL) atmosphere model AM3 (Donner et al., 2011) assumes a uniform PDF of total water as well. ~~While several~~

Several global atmosphere models including ECHAM6-HAM2 already make assumptions to account for the subgrid-scale variability of other atmospheric variables, e.g. for vertical velocity when computing droplet activation rates (Ghan et al., 1997; Lohmann et al., 2007; Golaz et al., 2011). However, subgrid-scale variability of RH or RH~~$_\mathrm{cls}$ is usually~~ $_\mathrm{cls}$ is not taken into account when computing hygroscopic growth of interstitial aerosols besides in some studies that made strong simplification regarding the shape and variation of the used PDF as explained in the introduction (Haywood et al., 1997; Haywood and Ramaswamy, 1998

2.3 ~~Stochastic parameterization for the subgrid-scale variability of clear-sky relative humidity~~

For ~~the stochastic parameterization~~ our stochastic parameterization of subgrid-scale variability of $\mathrm{RH_{cls}}$, we use the subsaturated part of the q_t-PDF from the cloud cover scheme in not-overcast cases (see Fig. 1a). This diagnosed PDF is transformed into a $\mathrm{RH_{cls}}$-PDF dividing it by q_s. Afterwards, it is sampled for the stochastic parameterization of subgrid-scale variability of $\mathrm{RH_{cls}}$. The width of the q_t-PDF in the cloud cover scheme is:

$$2\Delta q = 2\gamma q_\mathrm{s} = 2\cdot(1 - \mathrm{RH_{crit}})q_\mathrm{s} \tag{3}$$

Dividing Eq. (3) by q_s yields the width of the corresponding RH-PDF. For cloud-free grid-boxes this RH-PDF is equivalent to the $\mathrm{RH_{cls}}$-PDF. In this case, its which width is

$$2\Delta\mathrm{RH_{cls}} = 2\frac{\Delta q}{q_\mathrm{s}} = 2\cdot(1 - \mathrm{RH_{crit}}). \tag{4}$$

$\mathrm{RH_{crit}}$ is computed by Eq. (2)~~with values for $c_s = 0.9$, $c_t = 0.7$ and $n_\mathrm{x} = 4$ as used in the cloud cover scheme (Stevens et al., 2013)~~. However, when fractional cloud cover is present $\Delta\mathrm{RH_{cls}}$ has to be adjusted to

$$\Delta\mathrm{RH_{cls}} = \frac{q_\mathrm{s} - q_\mathrm{cls}}{q_\mathrm{s}} = 1 - \overline{\mathrm{RH}}_\mathrm{cls} \tag{5}$$

so that the variation of $\mathrm{RH_{cls}}$ occurs in the subsaturated part of the cloud cover PDF (see Fig. 1a).

Afterwards, instead of using $\overline{\mathrm{RH}}_\mathrm{cls}$ as input for the calculation of the gf, a stochastic value for clear-sky relative humidity, $\mathrm{RH_{cls,new}}$, from the inversion of the cumulative distribution function (CDF) is drawn (see Fig. 1b). For this, a random number,

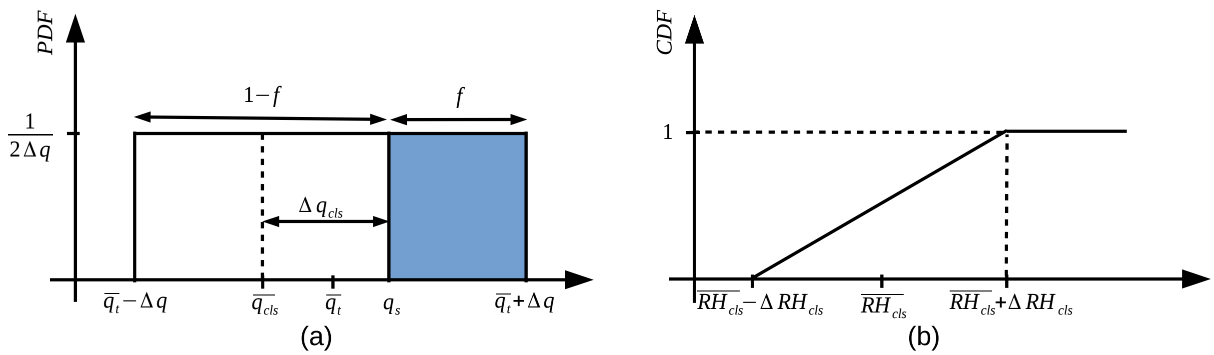

Figure 1. (a) Scheme for predicting fractional cloud cover, f, with a uniform PDF for the total-water q_{t}. The blue area indicates the fraction of a grid cell which is covered by clouds. $\Delta\mathrm{RH}_{\mathrm{cls}}$ is set to $\Delta q/q_s = 1-\mathrm{RH}_{\mathrm{crit}}$ for a PDF around $\overline{\mathrm{RH}}_{\mathrm{cls}}$ if no fractional cloud cover is present (not depicted) or set to $(q_{\mathrm{s}} - q_{\mathrm{cls}})/q_{\mathrm{s}} = 1 - \overline{\mathrm{RH}}_{\mathrm{cls}}$ if fractional cloud cover is present (in the figure shown in terms of specific humidity). (b) Cumulative distribution function (CDF) for a uniform PDF around $\overline{\mathrm{RH}}_{\mathrm{cls}}$. By the inversion of the CDF and with a random number $a \in [0,1]$ (see Eq. (6)), a value between $\mathrm{RH}_{\mathrm{cls}} - \Delta\mathrm{RH}_{\mathrm{cls}}$ and $\mathrm{RH}_{\mathrm{cls}} + \Delta\mathrm{RH}_{\mathrm{cls}}$ is sampled and used as the argument for the hygroscopic growth.

$a \in [0,1]$, is generated and inserted into the following equation:

$$\mathrm{RH}_{\mathrm{cls,new}} = \mathrm{RH}_{\mathrm{cls,old}}\overline{\mathrm{RH}}_{\mathrm{cls}} + \Delta\mathrm{RH}_{\mathrm{cls}}(2a-1). \tag{6}$$

Note, that the integration of the model is not fully deterministic in the current setting. If one preferred a deterministic model, one could configure the random number generator such that in reach integration the same random numbers are generated

2.3 Model settings and postprocessing

ECHAM-HAM2 is run with a resolution of T63L31. For aerosol emissions, the AEROCOM II data for 1850 for pre-industrial (PI) and for 2000 for present-day (PD) simulations are used (Lamarque et al. (2010); see section 7). Climatological sea surface temperature (SST) and sea ice distributions are prescribed. Ten-year model free-running (no nudging) simulations starting 1 January 2000 are performed with PI and PD aerosol emissions, both with and without the new parameterization.

~~The ERFari$_{\mathrm{cls}}$~~ The total ERF by anthropogenic aerosols, ERFaer, is computed by ~~the difference of the global mean net radiative balance under clear-sky conditions between the PD and the PI simulations.~~

$$\mathrm{ERFari}_{\mathrm{cls}} = (SW_{\mathrm{net,cls}} + LW_{\mathrm{net,cls}})_{PD} - (SW_{\mathrm{net,cls}} + LW_{\mathrm{net,cls}})_{PI}$$

~~In reality, clouds would mask part of this clear-sky ERF. Therefore, it should be considered as an idealised value.~~

$$\mathrm{ERFaer} = (SW_{\mathrm{net}} + LW_{\mathrm{net}})_{PD} - (SW_{\mathrm{net}} + LW_{\mathrm{net}})_{PI} \tag{7}$$

where the short and longwave radiative fluxes, SW and LW, are at the top of atmosphere (TOA). The radiative forcing due to aerosol-radiation interactions, RFari, is computed as suggested by Ghan (2013) :

$$\mathrm{RFari} = (SW_{\mathrm{net}} - SW_{\mathrm{net,clean}})_{PD} - (SW_{\mathrm{net}} - SW_{\mathrm{net,clean}})_{PI} \tag{8}$$

Again, radiative fluxes are at TOA. The subscript clean indicates the results of the radiative transfer equation for an atmosphere with no aerosols.

To depict changes in hygroscopic growth we define the squared ratio

$$\beta = \left(\frac{gf_{\,\mathrm{stoch}}}{gf_{\,\mathrm{control}}}\right)^2 \tag{9}$$

where $gf_{\,\mathrm{stoch}}$ and $gf_{\,\mathrm{control}}$ account for the growth factor in the model run with the stochastic parameterization and the control model run, respectively. The squared ratio scales with the effective extinction cross section and therefore describes the influence on aerosol optical depth (AOD).

Satellite retrievals of AOD from the MODerate Resolution Imaging Spectroradiometer (MODIS) platform Aqua (Levy et al., 2013) from the period between August 2002 and December 2010 are used to evaluate the results of implementing subgrid-scale variability of $\mathrm{RH_{cls}}$ into the model. The temporal mean values of AOD measurements ($\overline{\mathrm{AOD}}_{\mathrm{MODIS}}$) for the entire time span (08/2002 - 12/2010) are compared to the temporal means (01/2000 - 12/2009) of the model data ($\overline{\mathrm{AOD}}_{\mathrm{control}}$, $\overline{\mathrm{AOD}}_{\mathrm{stoch}}$). ~~However, differences between the model AOD with and without the new parameterization are small compared to differences between the AOD of both model runs and the AOD measured by MODIS-Aqua. In order to estimate if subgrid-scale variability improves the model performance on AOD we assess the change in absolute differences~~

$$c = |\overline{\mathrm{AOD}}_{\mathrm{stoch}} - \overline{\mathrm{AOD}}_{\mathrm{MODIS}}| - |\overline{\mathrm{AOD}}_{\mathrm{control}} - \overline{\mathrm{AOD}}_{\mathrm{MODIS}}|.$$

~~A value of c less than 0 implies that the implementation of subgrid-scale variability of $\mathrm{RH_{cls}}$ has improved the model skill to simulate AOD.~~

3 Results

In the following results from PD simulations, if not specified differently, are presented. ~~In~~ We compute uncertainties for a 95 %-confidence interval on basis of yearly mean values from the temporal variability. In differences, uncertainties are added in quadrature.

In Fig. 2a the global mean profiles of β are shown for ~~each~~ all soluble aerosol mode. Hygroscopic growth of aerosols is in general enhanced due to the implementation of a subgrid-scale variability of $\mathrm{RH_{cls}}$. We find that the effect is stronger for aerosol particles with a large particle radius. Thus, the effect is ~~stronger~~ strongest for particles from ~~CS and AS mode than~~ the CS mode (red line in Fig. 2a) and weakest for particles from ~~KS and NS mode~~ the NS mode (black line in Fig. 2a). Moreover, the effect on hygroscopic growth has a maximum between 700 hPa and 600 hPa for each aerosol mode.

The global mean AOD increases by 0.009 ± 0.002 ($\sim 7.8\,\%$). The response in AOD is weaker in simulations with PI emissions with a global mean difference of 0.006 ± 0.002 ($\sim 6.0\,\%$). ~~Here, uncertainties are computed for a 95-confidence interval on basis of yearly mean values from the temporal variability. In differences, uncertainties are added in quadrature.~~ Figure 3a shows that ~~, as expected,~~ the AOD increased especially in lower latitudes with a mean of about 0.013 in the tropics. Furthermore, the figure reveals that the AOD of diagnosed aerosol water (WAT) dominates the change in total AOD, not the change in dry matter of SS or SO4. Figure 3b shows the zonal mean AOD values from the model runs with and without the stochastic parameterization and from satellite measurements of MODIS-Aqua. Changes due to the new parameterization are small in comparison to the general difference between modelled and measured AOD. The ~~implementation of the subgrid-scale variability improves ($e < 0$) the model performance especially over land and areas with high anthropogenic emissions like East China and the East Coast of the United States. In contrast, model performance is worse ($e > 0$)over the Northern Atlantic Ocean, the Pacific around Hawaii and over most parts of the oceans in the southern hemisphere (not depicted). The global mean value of e is -0.001. This implies that the implemented parameterization has just a very small positive influence on modelled AOD ($\overline{\mathrm{AOD}}_{\mathrm{model}} \simeq 0.12$) with respect to AOD measurements from MODIS-Aqua.~~ absorption aerosol optical depth (AAOD) increased by $0.12 \pm 0.04 \cdot 10^{-3}$ (~ 4.7 %), mainly due to an increase in AAOD by BC of about $0.11 \cdot 10^{-3}$. However, note that in absolute terms the change of AOD is nearly two orders of magnitude greater than the change of AAOD.

Furthermore, the implementation of the new parameterization enhanced the ratio of scattering efficiency to total extinction efficiency, ω, for the CS, AS and KS aerosol mode with a maximum for the KS mode (2.6 %). ~~Therefore, more extinction occurs due to scattering.~~ The effective extinction cross section, σ, increases for the CS, AS and KS aerosol mode as well. The strongest change is visible for the KS mode with a change by 15.1 %. Note that no output for ω and σ is generated by the model for NS mode. Finally, the Ångström exponent for wet particles, α, changes by -0.8 $\cdot 10^{-3}$ ~~$\pm 11 \cdot 10^{-3}$. This confirms that particles are on average bigger in the model run with the stochastic parameterization than in the control model run.~~ $\pm 11.5 \cdot 10^{-3}$ (-0.11 %). The total cloud cover decreased by -0.08 ± 0.14% in PD simulations. In contrast, it increased by 0.17 ± 0.14 in PI simulations. The global mean profile of cloud cover f in Fig. 4 reveals a slight increase of cloud cover between 700 and 900 hPa for PD simulations, whereas it mainly decreased below and above this layer. However, in PI runs f increased for most parts of the atmosphere with a very little decrease at around 600 hPa.

In the following, solar and thermal clear-sky radiation represent the idealised solar and thermal irradiance that would arise from an atmosphere where clouds are absent, whereas all-sky stands for the irradiance that takes the effect of clouds into account. The net clear-sky solar radiation $SW_{\mathrm{net,cls}}$ decreases by $-0.22 \pm 0.07\,\mathrm{W\,m^{-2}}$. In addition, the net all-sky solar radiation SW_{net} changes by $-0.34 \pm 0.22\,\mathrm{W\,m^{-2}}$. For PI emissions, the effect on $SW_{\mathrm{net,cls}}$ is with a change of $-0.13 \pm 0.06\,\mathrm{W\,m^{-2}}$, as ~~anticipated~~expected, smaller than for PD emissions. In contrast, a stronger effect in PI runs than in PD runs is visible for SW_{net} ($-0.47 \pm 0.19\,\mathrm{W\,m^{-2}}$). Responses in the thermal radiation (positive downward) are small. The clear-sky thermal radiation $LW_{\mathrm{net,cls}}$ has a slight positive tendency with a mean value of $0.04 \pm 0.09\,\mathrm{W\,m^{-2}}$. Similar to solar radiation, the all-sky thermal radiation LW_{net} changes more than the clear-sky radiation with a global mean of $0.06 \pm 0.14\,\mathrm{W\,m^{-2}}$.

The comparison of ten-year model runs with PD and PI aerosol emissions reveals a change of the ~~$\mathrm{ERFari_{cls}}$ from -0.29 ± 0.09~~RFari from $-0.15 \pm 0.04\,\mathrm{W\,m^{-2}}$ to ~~-0.45 ± 0.11~~$-0.19 \pm 0.04\,\mathrm{W\,m^{-2}}$ (~~57~~31 %) in runs without ~~to~~ and runs with the new parameterization, respectively. This implies that subgrid-scale variability of $\mathrm{RH_{cls}}$ enhances the cooling effect of anthropogenic aerosol emissions by aerosol-radiation interactions in climate simulations. It is interesting to note that the ~~$\mathrm{ERFari_{cls}}$~~ RFari increases substantially given the relatively small impact of the revision on present-day TOA balance. This can be attributed to the fact that anthropogenic aerosol is disproportionally hygroscopic. Furthermore, the effect on ~~$\mathrm{ERFari_{cls}}$~~ RFari translates into the ERF of anthropogenic aerosols (ERFaer) that has as well a negative tendency (~~-0.07 ± 0.27). The total cloud cover decreased by~~

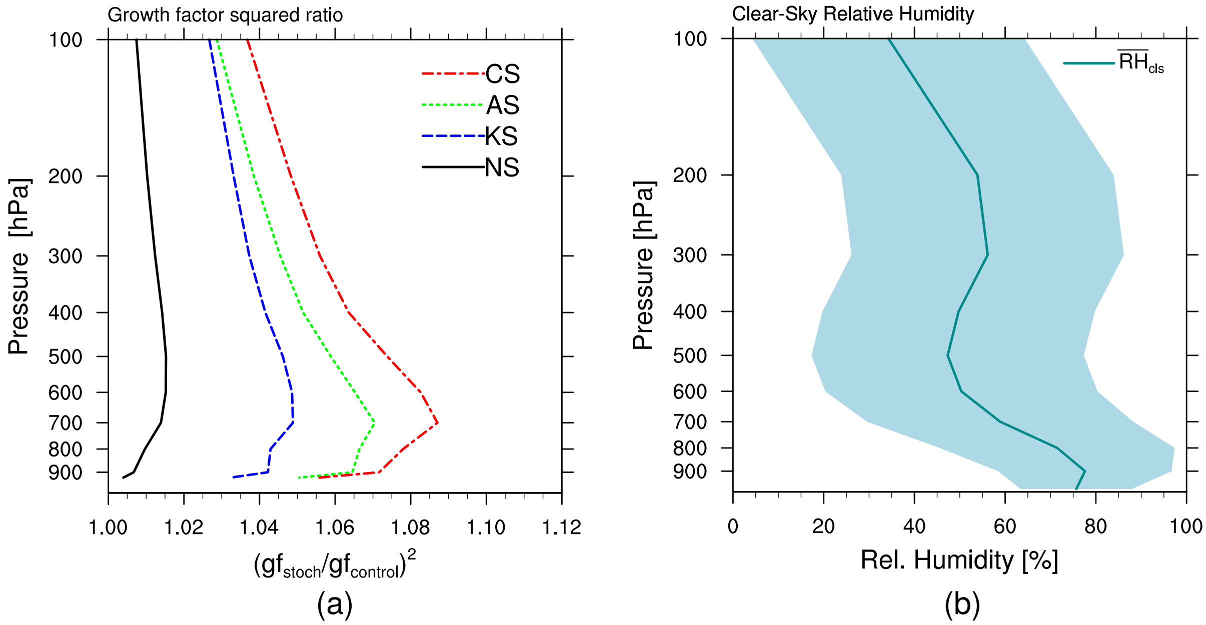

Figure 2. (a) Profile of the global mean of ~~β,~~ the squared ratio of the growth factor between the run with the stochastic parameterization of hygroscopic growth, gf_{stoch}, and the control run , gf_{control}. CS is the soluble Coarse aerosol mode (~~$r > 0.5$m~~red). AS the soluble Accumulation (~~$0.05 < r < 0.5$m~~green), KS the soluble Aitken (~~$0.005 < r < 0.05$m~~blue) and NS the soluble Nucleation aerosol mode (~~$r < 0.005$m~~black). (b) Profile of global mean clear-sky relative humidity (dark blue line) with its corresponding range of subgrid-scale variability (light blue area).

~~-0.08 ± 0.14in PD simulations. In contrast, it increased by 0.17 ± 0.14 in PI simulations. The global mean profile of cloud cover f in Fig. 4 reveals a slight increase of cloud cover between 700 and 900hPa for PD simulations, whereas it mainly decreased below and above this layer. However, in PI runs f increased for most parts of the atmosphere with a very little decrease at around 600hPa.~~ -0.07 ± 0.27). A summary of the influence of subgrid-scale variability of $\mathrm{RH_{cls}}$ on optical and radiative variables is given in Table 2.

4 Discussion

As for the previous section, we discuss in the following the results from PD simulations, if not specified differently. In model runs with the new parameterization aerosol particles swell stronger at each height level due to the non-linear nature of hygroscopic growth (see Eq. 1). The positive curvature of this function for $\mathrm{RH_{cls}} \in [0,1]$ implies that by applying a uniform PDF on $\mathrm{RH_{cls}}$ the expected value of $gf(\mathrm{RH_{cls}})$ is greater than $gf(\overline{\mathrm{RH}}_{\mathrm{cls}})$ with $\overline{\mathrm{RH}}_{\mathrm{cls}}$ being the grid box mean clear-sky relative humidity.

Effects are stronger for aerosol particles with a larger radius, and thus, particles from CS and AS mode. Three reasons can explain the vertical shape of the gf-profiles:

Table 2. Changes of global mean values of optical and radiative variables due to the implementation of subgrid-scale variability of RH_{cls} are listed. Uncertainties of the mean value are calculated for a 95 %-confidence interval on basis of yearly mean values from the temporal variability. Uncertainties of differences are added in quadrature. ω is the ratio of the scattering efficiency to the total extinction efficiency and σ the effective extinction cross section. The indices KS, AS and CS ~~stand for~~ indicate Aitken, Accumulation and Coarse mode. α is the wet Ångström exponent, SW_{net} the net short wave radiation and with index $SW_{net,cls}$ the net short wave radiation in the clear-sky part. With the same meaning for the indices LW is the longwave radiation. TCC is the total cloud cover. Results are presented for present-day and pre-industrial emissions.

Variable	Stoch	Control	Difference	Relative deviation
~~$ERFari_{cls}$~~ RFari [$W\,m^{-2}$]	~~-0.45 ± 0.11~~ -0.19 ± 0.04	~~-0.29 ± 0.09~~ -0.15 ± 0.04	~~-0.16 ± 0.14~~ -0.04 ± 0.06	~~57~~31%
ERFaer [$W\,m^{-2}$]	-1.52 ± 0.16	-1.45 ± 0.21	-0.07 ± 0.27	5%

	Present-Day		Pre-Industrial	
Variable	Difference	Relative deviation	Difference	Relative deviation
SW_{net} [$W\,m^{-2}$]	-0.34 ± 0.22	-0.15 %	-0.47 ± 0.19	-0.20 %
$SW_{net,cls}$ [$W\,m^{-2}$]	-0.22 ± 0.07	-0.08 %	-0.13 ± 0.06	-0.05 %
LW_{net} [$W\,m^{-2}$]	0.06 ± 0.14	0.03 %	0.26 ± 0.17	0.10 %
$LW_{net,cls}$ [$W\,m^{-2}$]	0.04 ± 0.09	0.02 %	0.11 ± 0.10	0.04 %
TCC [%]	-0.08 ± 0.14	-0.13 %	0.17 ± 0.14	0.26 %
AOD	0.009 ± 0.002	7.8 %	0.006 ± 0.002	6.0 %
AOD_{WAT}	0.008 ± 0.001	9.5 %	0.005 ± 0.001	7.8 %
$AAOD$	$(0.12 \pm 0.04) \cdot 10^{-3}$	4.7 %	$(0.04 \pm 0.03) \cdot 10^{-3}$	2.7 %
$AAOD_{BC}$	$(0.11 \pm 0.03) \cdot 10^{-3}$	5.1 %	$(0.03 \pm 0.01) \cdot 10^{-3}$	3.4 %
ω_{KS}	0.015 ± 0.003	2.64 %	0.014 ± 0.005	2.42 %
ω_{AS}	$(1.1 \pm 0.4) \cdot 10^{-3}$	0.11 %	$(0.9 \pm 0.6) \cdot 10^{-3}$	0.10 %
ω_{CS}	$(0.03 \pm 0.05) \cdot 10^{-3}$	0.003 %	$(0.05 \pm 0.15) \cdot 10^{-3}$	0.005 %
σ_{KS}	$(9.7 \pm 1.0) \cdot 10^{-18}$	15.1 %	$(8.0 \pm 1.1) \cdot 10^{-18}$	14.3 %
σ_{AS}	$(20.8 \pm 6.9) \cdot 10^{-15}$	4.5 %	$(22.7 \pm 7.2) \cdot 10^{-15}$	4.8 %
σ_{CS}	$(0.69 \pm 0.07 \cdot 10^{-12}$	3.9 %	$(0.71 \pm 0.07) \cdot 10^{-12}$	4.0 %
α	$(-0.8 \pm 11.5) \cdot 10^{-3}$	-0.11 %	$(6.4 \pm 13.8) \cdot 10^{-3}$	0.94 %

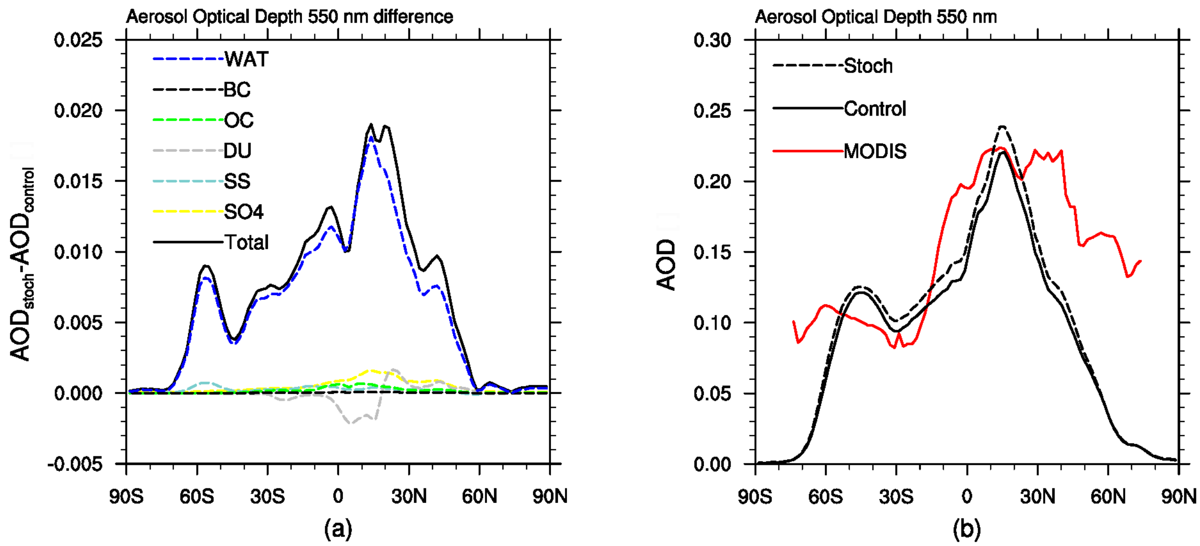

Figure 3. (a) Difference in AOD between the stochastic variation and the control run in AOD for different aerosol constituents. AOD from diagnosed aerosol water (WAT, blue) dominates the changes. (b) Temporally and zonally averaged clear-sky AOD ~~(computed from on monthly mean values)~~ from the control (plain) and stochastic (dashed) model runs (black, 01/2000 - 12/2009) and MODerate Resolution Imaging Spectroradiometer (Levy et al., 2013) Aqua satellite data (red, 08/2002 - 12/2010) is shown. Two discrepancies arise, namely (i) the fact that the model diagnoses clear-sky AOD also in overcast grid cells, with a relative humidity of RH=1 in these cases, which are dismissed in the MODIS retrieval, and (ii) the point that MODIS uses a conservative cloud masking, i.e. excludes pixels near cloud edges, whereas the model uses all clear-sky pixels.

(1) Clear-sky relative humidity has a decreasing trend with height in the model (see Fig. 2b). The same change ~~of RH_{cls}~~ ΔRH_{cls} in a drier environment leads to a smaller change in gf than in a more humid environment (unless saturation is reached) because of the non-linearity of Eq. (1)~~and therefore leads to smaller slopes of gf(RH) in the drier~~. The effect of the subgrid-scale variability of RH_{cls} on gf is therefore stronger in a more humid environment.

(2) Very hygroscopic aerosol particles are more sensitive to changes in relative humidity and larger particles tend to become deposited by impaction and sedimentation more easily. The main hygroscopic aerosol types are sulphate and sea salt, where sea salt (κ = 1.12) is more hygroscopic than sulphate (κ = 0.6). Sea salt particles are emitted at the surface of the ocean. Due to their high κ value, sea salt particles grow strongly, are deposited easily and can not reach high altitudes. ~~Therefore~~This is indicated in Fig. 4b that shows that the mixing ratio of sea salt decreases noticeably stronger with height than other aerosol compounds. Hence, the aerosol composition of the atmosphere shifts towards less hygroscopic components (smaller κ values) with height and the effect of perturbing relative humidity on hygroscopic growth becomes weaker with smaller κ values. ~~Pringle et al. (2010) examined~~ This is supported by the study of Pringle et al. (2010) that examines the global distribution of κ ~~and found~~ using the the ECHAM/MESSy Atmospheric Chemistry (EMAC) model. They find that especially at marine sites κ-values decrease with height, whereas at continental sites κ tends to be more constant with height. ~~However,~~

(1) and (2) can only explain a decreasing trend of β with height but not the maxima of the β profiles between 600 and 700 hPa.

(3) The critical relative humidity determines the width of the PDF which is used to vary $\mathrm{RH_{cls}}$ stochastically. The width $2\Delta\mathrm{RH_{cls}}$ of the PDF is calculated by ~~$\Delta\mathrm{RH_{cls}} = 1 - \mathrm{RH}_{crit}$~~ $\Delta\mathrm{RH_{cls}} = 1 - \mathrm{RH_{crit}}$ as described in section 2. But ~~RH_{crit}~~ $\mathrm{RH_{crit}}$ is a function of height (see Eq. (2)). It decreases from the surface to 600 hPa from 0.9 to close to 0.7. For higher altitudes, it is nearly constant and ~~just~~ converges slowly towards 0.7 (see Fig. 2b). This in fact means that the width of the PDF increases with height from the surface to 600 hPa. Then, it is almost constant. The positive curvature of Eq. ~~() implies that mean hygroscopic growth is stronger~~ (1) implies that the wider the PDF is the stronger the mean hygroscopic growth. The increasing width of the PDF explains why β becomes greater with height until 600 hPa. Above, ~~the two other effects~~ effect (1) and (2) are dominant and β decreases again.

The AOD, the effective extinction cross section, σ, and the ratio of scattering efficiency to total extinction efficiency, ω, are enhanced because of the increase in the geometrical radius of the particles. Anthropogenic aerosols that arise in PD simulations are disproportionally hygroscopic. Therefore, hygroscopic aerosols swell stronger due to the new parameterization in PD than in PI simulations and scatter more solar radiation. This leads in turn to a higher AOD in PD than PI runs. ~~As~~ The effect of the new parameterization is especially strong for lower latitudes because of the higher abundance of sea salt (not depicted) in these regions. In addition, anthropogenic emissions of sulphate are strong in China, India and over the Arab Peninsula and contribute to the peak of increased AOD in the northern tropics. Note, that ECHAM6-HAM2 currently does not simulate nitrate aerosols. The integration of nitrate aerosols will introduce very hygroscopic aerosols into the model that would alter our results. As Fig. 3b demonstrates, little can be said about improved skill of ECHAM-HAM2 to model AOD in respect to AOD satellite retrievals of MODIS-Aqua. ~~However, there is a hint at a slight improvement especially over land when including the subgrid-scale variability of~~ ~~$\mathrm{RH_{cls}}$.~~

The net clear-sky solar radiation $SW_{\mathrm{net,cls}}$ decreases ($\Delta SW_{\mathrm{net,cls}} = -0.22\,\mathrm{W\,m^{-2}}$) due to an increased reflection of solar radiation as indicated by an increased ω. However, the effect on the net all-sky solar radiation SW_{net} is greater ($\Delta SW_{\mathrm{net}} = -0.34\,\mathrm{W\,m^{-2}}$) than the effect on the net clear-sky solar radiation. This is maybe due to the fact that although total cloud cover (TCC) decreased by -0.08%, cloud cover ~~in~~ is slightly enhanced in height levels between about 700 and 900 hPa (see graph for PD in Fig. 4). Hence, more solar radiation is reflected back to space by these clouds.

We proceed with the discussion of differences that arise between PD and PI simulations. The change in $SW_{\mathrm{net,cls}}$ is stronger for PD than for PI emissions because backscattering of solar radiation is more enhanced by the new parameterization in PD than in PI simulations ~~as already explained. Because effects on~~ ~~$LW_{\mathrm{net,cls}}$~~ ~~are in general small, this translates as well into a strong response in~~ ~~$\mathrm{ERFari_{cls}}$. In contrast~~ because anthropogenic aerosols are disproportionally hygroscopic. In addition, the response in RFari ($-0.04\,\mathrm{W\,m^{-2}}$, 31 %), indicates as well that the parameterization leads to stronger backscattering by aerosols. Unexpectedly, the response in SW_{net} ~~was~~ is greater in PI runs ($\Delta SW_{\mathrm{net,PI}} = -0.47\,\mathrm{W\,m^{-2}}$) than in PD runs ($\Delta SW_{\mathrm{net,PD}} = -0.34\,\mathrm{W\,m^{-2}}$). We assume that this might be due to the enhanced total cloud cover in the PI simulations ($\Delta TCC_{\mathrm{PI}} = 0.17$) whereas total cloud cover decreased in PD simulations ($\Delta TCC_{\mathrm{PD}} = -0.08$). ~~However, cloud cover between 700 and 900hPa increased stronger in PD than in PI simulations (see Fig. 4). This slightly weakens the hypothesis that clouds caused a stronger~~

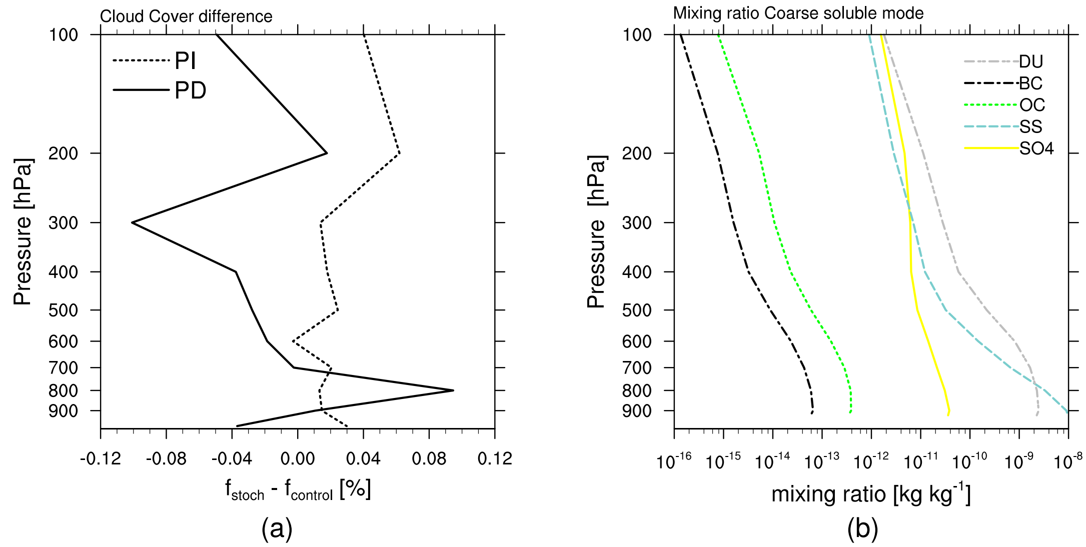

Figure 4. (a) Difference in cloud cover, f, due to the implementation of subgrid-scale variability of $\mathrm{RH_{cls}}$ for PI (dashed) and PD (solid) simulations. (b) Global mean profile of mass mixing ratio for various aerosol compounds from the CS mode.

~~decrease in~~ We ascribe the differences in cloud cover to internal variability. Hence, we suspect that the converse results for SW_{net} ~~in PI than in PD simulations, since low-level clouds are known to have a cooling effect on the radiative balance of the Earth (Hartmann et al., 1992; Chen et al., 2000) .~~

arise due to internal variability. The stronger increase in cloud cover for the higher troposphere in PI simulations (see Fig. 4) might explain the strong response LW_{net} in PI simulations ($\Delta LW_{\mathrm{net,PI}} = 0.26\,\mathrm{W\,m^{-2}}$). High-thin clouds, namely Cirrus clouds, are known to have positive effect on outgoing longwave radiation (Hartmann et al., 1992; Chen et al., 2000).

5 Conclusions

This study ~~investigated the effect of implementing~~ proposes a stochastic parameterization ~~for subgrid-scale variability~~ of clear-sky relative humidity ~~$\mathrm{RH_{cls}}$~~ that is consistent with the cloud cover scheme for its application in the aerosol hygroscopic growth parameterization. We investigate its effect on hygroscopic growth of aerosol particles as well as the subsequent changes of optical properties of the atmosphere and the radiative balance of the Earth. The implementation of the new parameterization ~~led~~ leads to stronger swelling of aerosol particles (as expected) and therefore ~~increased~~ increases the AOD ($\sim 7.8\,\%$). Furthermore, the increased AOD ~~caused~~ causes stronger backscattering of solar radiation under clear-sky conditions $SW_{\mathrm{net,cls}}$ ($-0.08\,\%$). Most importantly, the revision ~~had~~ has a very strong influence on the simulated ~~effective~~ radiative forcing due to aerosol-radiation interaction ~~under clear-sky conditions $\mathrm{ERFari_{cls}}$ (57~~RFari (31 %). In earlier studies RFari by sulphate increased in GCMs by ~~9-10~~about 10% when an idealized distributions for RH was implemented (Haywood and Shine, 1997; Haywood and Ramaswamy, 1998). Further studies found that GCMs underestimate RFari of sulphate when subgrid-scale variability of RH is not taken into account by 73 % in a limited-area-model case study (Haywood et al., 1997), by 30 to 80 % in a study that used a cloud-resolving model over a tropical ocean and a mid-latitude continental region (Petch, 2001) and by 30 to 40 % in a regional study (Europe and much of the North Atlantic) with a high resolution model (Myhre et al., 2002). Hence, our study is in accordance with previous investigations.

~~The comparison with satellite data reveals that the new parameterization performs better in areas where sulphate is the dominant soluble aerosol type. This is especially the case over land and in areas with high anthropogenic aerosol (precursor) emissions. In contrast, model performance is worse where sea salt is the main aerosol types. This occurs maybe due to the fact that sea salt fluxes are still not represented well enough in ECHAM6-HAM2.~~ One might be able to further improve the parameterization of subgrid-scale variability of RH_{cls} by applying the subsaturated part of the β-function from the optional Tompkins (2002) cloud cover scheme that prognostically treats the total-water variability PDF. Furthermore, Figure 2 in Quaas (2012) indicates that the critical relative humidity, RH_{crit}, that defines the width of the introduced RH_{cls}-PDF, varies horizontally in the same scale as vertically. Therefore, the width of the RH_{cls}-PDF could be extended from just height dependent to height and zonal or even height, zonal and meridional dependent.

6 Code availability

The ~~changed model code~~ code for the subgrid-scale variability of RH_{cls} is available upon request from the first author.

7 Data availability

The ECHAM6-HAM2 model output data used in this study is archived at the Leipzig Institute for Meteorology and is available upon request from the authors. Satellite data from MODIS-Aqua can be obtained at https://neo.sci.gsfc.nasa.gov/. AEROCOM emission data can be downloaded at http://aerocom.met.no/emissions.html.

Acknowledgements. The ECHAM-HAM model is developed by a consortium composed of ETH Zurich, Max Planck Institut für Meteorologie, Forschungszentrum Jülich, University of Oxford, the Finnish Meteorological Institute and the Leibniz Institute for Tropospheric Research, and managed by the Center for Climate Systems Modeling (C2SM) at ETH Zurich. The MODIS data are from the NASA Goddard Space Flight Center (ftp://laadsweb.nascom.nasa.gov). The CERES data were obtained from the Atmospheric Sciences Data Center at NASA Langley Research Center (http://ceres.larc.nasa.gov). Funding by the European Research Council in Starting Grant, grant agreement FP7-306284 (QUAERERE) is acknowledged.

References

Beer, A.: Bestimmung der Absorption des rothen Lichts in farbigen Flüssigkeiten, Annalen der Physik, 162, 78–88, 1852.

Berner, J., Achatz, U., Batté, L., Bengtsson, L., Cámara, A. d. l., Christensen, H. M., Colangeli, M., Coleman, D. R. B., Crommelin, D., Dolaptchiev, S. I., Franzke, C. L. E., Friederichs, P., Imkeller, P., Järvinen, H., Juricke, S., Kitsios, V., Lott, F., Lucarini, V., Mahajan, S., Palmer, T. N., Penland, C., Sakradzija, M., von Storch, J.-S., Weisheimer, A., Weniger, M., Williams, P. D., and Yano, J.-I.: Stochastic Parameterization: Toward a New View of Weather and Climate Models, Bull. Amer. Meteor. Soc., 98, 565–588, doi:10.1175/BAMS-D-15-00268.1, 2016.

Bond, T. C., Doherty, S. J., Fahey, D. W., Forster, P. M., Berntsen, T., DeAngelo, B. J., Flanner, M. G., Ghan, S., Kärcher, B., Koch, D., Kinne, S., Kondo, Y., Quinn, P. K., Sarofim, M. C., Schultz, M. G., Schulz, M., Venkataraman, C., Zhang, H., Zhang, S., Bellouin, N., Guttikunda, S. K., Hopke, P. K., Jacobson, M. Z., Kaiser, J. W., Klimont, Z., Lohmann, U., Schwarz, J. P., Shindell, D., Storelvmo, T., Warren, S. G., and Zender, C. S.: Bounding the role of black carbon in the climate system: A scientific assessment, J. Geophys. Res. Atmos., 118, 5380–5552, doi:10.1002/jgrd.50171, 2013.

Boucher, O., Randall, D., Artaxo, P., Bretherton, C., Feingold, G., Forster, P., Kerminen, V.-M., Kondo, Y., Liao, H., Lohmann, U., et al.: Clouds and aerosols, in: Climate change 2013: The physical science basis. Contribution of working group I to the fifth assessment report of the intergovernmental panel on climate change, pp. 571–657, Cambridge University Press, 2013.

Chen, T., Rossow, W. B., and Zhang, Y.: Radiative Effects of Cloud-Type Variations, J. Climate, 13, 264–286, doi:10.1175/1520-0442(2000)013<0264:REOCTV>2.0.CO;2, 2000.

Chýlek, P., Lesins, G. B., Videen, G., Wong, J. G. D., Pinnick, R. G., Ngo, D., and Klett, J. D.: Black carbon and absorption of solar radiation by clouds, J. Geophys. Res., 101, 23 365–23 371, doi:10.1029/96JD01901, 1996.

Donner, L. J., Wyman, B. L., Hemler, R. S., Horowitz, L. W., Ming, Y., Zhao, M., Golaz, J.-C., Ginoux, P., Lin, S.-J., Schwarzkopf, D. M., Austin, J., Alaka, G., Cooke, W. F., Delworth, T. L., Freidenreich, S. M., Gordon, C. T., Griffies, S. M., Held, I. M., Hurlin, W. J., Klein, S. A., Knutson, T. R., Langenhorst, A. R., Lee, H.-C., Lin, Y., Magi, B. I., Malyshev, S. L., Milly, P. C. D., Naik, V., Nath, M. J., Pincus, R., Ploshay, J. J., Ramaswamy, V., Seman, C. J., Shevliakova, E., Sirutis, J. J., Stern, W. F., Stouffer, R. J., Wilson, R. J., Winton, M., Wittenberg, A. T., and Zeng, F.: The dynamical core, physical parameterizations, and basic simulation characteristics of the atmospheric component AM3 of the GFDL global coupled model CM3, 24, 3484–3519, doi:10.1175/2011JCLI3955.1, 2011.

Ghan, S. J.: Technical Note: Estimating aerosol effects on cloud radiative forcing, Atmos. Chem. Phys., 13, 9971–9974, doi:10.5194/acp-13-9971-2013, 2013.

Ghan, S. J. and Zaveri, R. A.: Parameterization of optical properties for hydrated internally mixed aerosol, J. Geophys. Res., 112, D10 201, doi:10.1029/2006JD007927, 2007.

Ghan, S. J., Leung, L. R., Easter, R. C., and Abdul-Razzak, H.: Prediction of cloud droplet number in a general circulation model, J. Geophys. Res., 102, 21 777–21 794, 1997.

Ginoux, P.: Atmospheric chemistry: Warming or cooling dust?, Nature Geosci, 10, 246–248, doi:10.1038/ngeo2923, 2017.

Golaz, J.-C., Salzmann, M., Donner, L. J., Horowitz, L. W., Ming, Y., and Zhao, M.: Sensitivity of the aerosol indirect effect to subgrid variability in the cloud parameterization of the GFDL Atmosphere General Circulation Model AM3, J. Clim., 24, doi:10.1175/2010JCLI3945.1, 2011.

Gustafson, W. I., Qian, Y., and Fast, J. D.: Downscaling aerosols and the impact of neglected subgrid processes on direct aerosol radiative forcing for a representative global climate model grid spacing, J. Geophys. Res., 116, D13 303, doi:10.1029/2010JD015480, 2011.

Haarig, M., Ansmann, A., Gasteiger, J., Kandler, K., Althausen, D., Baars, H., Radenz, M., and Farrell, D. A.: Dry versus wet marine particle optical properties: RH dependence of depolarization ratio, backscatter, and extinction from multiwavelength lidar measurements during SALTRACE, Atmos. Chem. Phys., 17, 14 199–14 217, doi:10.5194/acp-17-14199-2017, 2017.

Hartmann, D. L., Ockert-Bell, M. E., and Michelsen, M. L.: The Effect of Cloud Type on Earth's Energy Balance: Global Analysis, J. Climate, 5, 1281–1304, doi:10.1175/1520-0442(1992)005<1281:TEOCTO>2.0.CO;2, 1992.

Haywood, J. M. and Ramaswamy, V.: Global sensitivity studies of the direct radiative forcing due to anthropogenic sulfate and black carbon aerosols, J. Geophys. Res., 103, 6043–6058, doi:10.1029/97JD03426, 1998.

Haywood, J. M. and Shine, K. P.: Multi-spectral calculations of the direct radiative forcing of tropospheric sulphate and soot aerosols using a column model, Q.J.R. Meteorol. Soc., 123, 1907–1930, doi:10.1002/qj.49712354307, 1997.

Haywood, J. M., Ramaswamy, V., and Donner, L. J.: A limited-area-model case study of the effects of sub-grid scale Variations in relative humidity and cloud upon the direct radiative forcing of sulfate aerosol, Geophys. Res. Lett., 24, 143–146, doi:10.1029/96GL03812, 1997.

Jacobson, M. Z.: Investigating cloud absorption effects: Global absorption properties of black carbon, tar balls, and soil dust in clouds and aerosols, J. Geophys. Res., 117, D06 205, doi:10.1029/2011JD017218, 2012.

Köhler, H.: The nucleus in and the growth of hygroscopic droplets, Trans. Faraday Soc., 32, 1152–1161, doi:10.1039/TF9363201152, 1936.

Lamarque, J.-F., Bond, T. C., Eyring, V., Granier, C., Heil, A., Klimont, Z., Lee, D., Liousse, C., Mieville, A., Owen, B., et al.: Historical (1850–2000) gridded anthropogenic and biomass burning emissions of reactive gases and aerosols: methodology and application, Atmospheric Chemistry and Physics, 10, 7017–7039, 2010.

Lambert, J. H.: Photometria, sive de Mensura et Gradibus Luminis, Colorum et Umbrae, VE Klett Augustae Vindelicorum, 1760.

Levy, R. C., Mattoo, S., Munchak, L. A., Remer, L. A., Sayer, A. M., Patadia, F., and Hsu, N. C.: The Collection 6 MODIS aerosol products over land and ocean, Atmos. Meas. Tech., 6, 2989–3034, doi:10.5194/amt-6-2989-2013, 2013.

Liu, L., Mishchenko, M. I., Menon, S., Macke, A., and Lacis, A. A.: The effect of black carbon on scattering and absorption of solar radiation by cloud droplets, Journal of Quantitative Spectroscopy and Radiative Transfer, 74, 195–204, doi:10.1016/S0022-4073(01)00232-1, 2002.

Lohmann, U., Stier, P., Hoose, C., Ferrachat, S., Kloster, S., Roeckner, E., and Zhang, J.: Cloud microphysics and aerosol indirect effects in the global climate model ECHAM5-HAM, 7, 3425–3446, 2007.

Mie, G.: Beiträge zur Optik trüber Medien, speziell kolloidaler Metallösungen, Annalen der physik, 330, 377–445, 1908.

Myhre, G., Jonson, J. E., Bartnicki, J., Stordal, F., and Shine, K. P.: Role of spatial and temporal variations in the computation of radiative forcing due to sulphate aerosols: A regional study, Q.J.R. Meteorol. Soc., 128, 973–989, doi:10.1256/0035900021643610, 2002.

Myhre, G., Samset, B. H., Schulz, M., Balkanski, Y., Bauer, S., Berntsen, T. K., Bian, H., Bellouin, N., Chin, M., Diehl, T., Easter, R. C., Feichter, J., Ghan, S. J., Hauglustaine, D., Iversen, T., Kinne, S., Kirkevåg, A., Lamarque, J.-F., Lin, G., Liu, X., Lund, M. T., Luo, G., Ma, X., van Noije, T., Penner, J. E., Rasch, P. J., Ruiz, A., Seland, o., Skeie, R. B., Stier, P., Takemura, T., Tsigaridis, K., Wang, P., Wang, Z., Xu, L., Yu, H., Yu, F., Yoon, J.-H., Zhang, K., Zhang, H., and Zhou, C.: Radiative forcing of the direct aerosol effect from AeroCom Phase II simulations, Atmospheric Chemistry and Physics, 13, 1853–1877, doi:10.5194/acp-13-1853-2013, 2013.

Petch, J. C.: Using a cloud-resolving model to study the effects of subgrid-scale variations in relative humidity on direct sulphate-aerosol forcing, Q.J.R. Meteorol. Soc., 127, 2385–2394, doi:10.1002/qj.49712757710, 2001.

Petters, M. D. and Kreidenweis, S. M.: A single parameter representation of hygroscopic growth and cloud condensation nucleus activity, Atmos. Chem. Phys., 7, 1961–1971, doi:10.5194/acp-7-1961-2007, 2007.

Pringle, K. J., Tost, H., Pozzer, A., Pöschl, U., and Lelieveld, J.: Global distribution of the effective aerosol hygroscopicity parameter for CCN activation, Atmos. Chem. Phys., 10, 5241–5255, doi:10.5194/acp-10-5241-2010, 2010.

Quaas, J.: Evaluating the "critical relative humidity" as a measure of subgrid-scale variability of humidity in general circulation model cloud cover parameterizations using satellite data, J. Geophys. Res., 117, D09 208, doi:10.1029/2012JD017495, 2012.

Rosch, J., Heus, T., Brueck, M., Salzmann, M., Mülmenstädt, J., Schlemmer, L., and Quaas, J.: Analysis of diagnostic climate model cloud parametrizations using large-eddy simulations, Q.J.R. Meteorol. Soc., 141, 2199–2205, doi:10.1002/qj.2515, 2015.

Shindell, D. T., Lamarque, J.-F., Schulz, M., Flanner, M., Jiao, C., Chin, M., Young, P. J., Lee, Y. H., Rotstayn, L., Mahowald, N., Milly, G., Faluvegi, G., Balkanski, Y., Collins, W. J., Conley, A. J., Dalsoren, S., Easter, R., Ghan, S., Horowitz, L., Liu, X., Myhre, G., Nagashima, T., Naik, V., Rumbold, S. T., Skeie, R., Sudo, K., Szopa, S., Takemura, T., Voulgarakis, A., Yoon, J.-H., and Lo, F.: Radiative forcing in the ACCMIP historical and future climate simulations, Atmos. Chem. Phys., 13, 2939–2974, doi:10.5194/acp-13-2939-2013, 2013.

Skupin, A., Ansmann, A., Engelmann, R., Seifert, P., and Müller, T.: Four-year long-path monitoring of ambient aerosol extinction at a central European urban site: dependence on relative humidity, Atmos. Chem. Phys., 16, 1863–1876, doi:10.5194/acp-16-1863-2016, 2016.

Stevens, B., Giorgetta, M., Esch, M., Mauritsen, T., Crueger, T., Rast, S., Salzmann, M., Schmidt, H., Bader, J., Block, K., Brokopf, R., Fast, I., Kinne, S., Kornblueh, L., Lohmann, U., Pincus, R., Reichler, T., and Roeckner, E.: Atmospheric component of the MPI-M Earth System Model: ECHAM6, J. Adv. Model. Earth Syst., 5, 146–172, doi:10.1002/jame.20015, 2013.

Stier, P., Feichter, J., Kinne, S., Kloster, S., Vignati, E., Wilson, J., Ganzeveld, L., Tegen, I., Werner, M., Balkanski, Y., Schulz, M., Boucher, O., Minikin, A., and Petzold, A.: The aerosol-climate model ECHAM5-HAM, Atmos. Chem. Phys., 5, 1125–1156, doi:10.5194/acp-5-1125-2005, 2005.

Stier, P., Seinfeld, J. H., Kinne, S., Feichter, J., and Boucher, O.: Impact of nonabsorbing anthropogenic aerosols on clear-sky atmospheric absorption, J. Geophys. Res., 111, D18 201, doi:10.1029/2006JD007147, 2006.

Stier, P., Seinfeld, J. H., Kinne, S., and Boucher, O.: Aerosol absorption and radiative forcing, Atmospheric Chemistry and Physics, 7, 5237–5261, 2007.

Sundqvist, H., Berge, E., and Kristjánsson, J. E.: Condensation and cloud parameterization studies with a mesoscale numerical weather prediction model, Monthly Weather Review, 117, 1641–1657, 1989.

Tiedtke, M.: Representation of clouds in large scale models, Mon. Weather Rev., 121, 3040–3061, 1993.

Tompkins, A. M.: A Prognostic Parameterization for the Subgrid-Scale Variability of Water Vapor and Clouds in Large-Scale Models and Its Use to Diagnose Cloud Cover, J. Atmos. Sci., 59, 1917–1942, doi:10.1175/1520-0469(2002)059<1917:APPFTS>2.0.CO;2, 2002.

Tompkins, A. M. and Berner, J.: A stochastic convective approach to account for model uncertainty due to unresolved humidity variability, J. Geophys. Res., 113, D18 101, doi:10.1029/2007JD009284, 2008.

Toon, O. B. and Ackerman, T. P.: Algorithms for the calculation of scattering by stratified spheres, Applied Optics, 20, 3657, doi:10.1364/AO.20.003657, 1981.

Twohy, C. H., Clarke, A. D., Warren, S. G., Radke, L. F., and Charlson, R. J.: Light-absorbing material extracted from cloud droplets and its effect on cloud albedo, J. Geophys. Res., 94, 8623–8631, doi:10.1029/JD094iD06p08623, 1989.

Vignati, E., Wilson, J., and Stier, P.: M7: An efficient size-resolved aerosol microphysics module for large-scale aerosol transport models, J. Geophys. Res., 109, D22 202, doi:10.1029/2003JD004485, 2004.

Weigum, N., Schutgens, N., and Stier, P.: Effect of aerosol subgrid variability on aerosol optical depth and cloud condensation nuclei: implications for global aerosol modelling, Atmos. Chem. Phys., 16, 13 619–13 639, doi:10.5194/acp-16-13619-2016, 2016.

Zhang, K., O'Donnell, D., Kazil, J., Stier, P., Kinne, S., Lohmann, U., Ferrachat, S., Croft, B., Quaas, J., Wan, H., Rast, S., and Feichter, J.: The global aerosol-climate model ECHAM-HAM, version 2: sensitivity to improvements in process representations, Atmos. Chem. Phys., 12, 8911–8949, doi:10.5194/acp-12-8911-2012, 2012.

Zieger, P., Fierz-Schmidhauser, R., Weingartner, E., and Baltensperger, U.: Effects of relative humidity on aerosol light scattering: results from different European sites, Atmos. Chem. Phys., 13, 10 609–10 631, doi:10.5194/acp-13-10609-2013, 2013.